Homeostatic scaling is driven by a translation-dependent degradation axis that recruits miRISC remodeling

Balakumar Srinivasan[1#], Sarbani Samaddar[1#], Sivaram V.S. Mylavarapu[2], James P. Clement[3] and Sourav Banerjee[1§]

1. National Brain Research Centre, NH-8. Nainwal Mode, Manesar-122052, Haryana, India

2. Regional Centre for Biotechnology, NCR-Biotech Science Cluster, Faridabad-Gurgaon Expressway, Faridabad-121001, Haryana, India

3. Neuroscience Unit, Jawaharlal Nehru Centre for Avanced Scientific Research, Jakkur, Bengaluru-560064, Karnataka, India.

# These authors contributed equally to this work

§ Correspondence

souravnbrc@gmail.com OR sourav@nbrc.ac.in (S.B)

Abstract

Homeostatic scaling in neurons has been attributed to the individual contribution of either translation or degradation; however there remains limited insight towards understanding how the interplay between the two processes effectuates synaptic homeostasis. Here, we report that a co-dependence between protein synthesis and degradation mechanisms drives synaptic homeostasis whereas abrogation of either prevents it. Coordination between the two processes is achieved through the formation of a tripartite complex between translation regulators, the 26S proteasome and the miRNA-induced-silencing-complex (miRISC) components such as Argonaute, MOV10 and Trim32 on actively translating transcripts or polysomes. The components of this ternary complex directly interact with each other in an RNA-dependent manner. Disruption of polysomes abolishes this ternary interaction, suggesting that translating RNAs facilitate the combinatorial action of the proteasome and the translational apparatus. We identify that synaptic downscaling involves miRISC remodeling which entails the mTORC1-dependent translation of Trim32, an E3 ligase and the subsequent degradation of its target, MOV10 *via* the phosphorylation of p70 S6 kinase. We find that the E3 ligase Trim32 specifically polyubiquitinates MOV10 for its degradation during synaptic downscaling. MOV10 degradation alone is sufficient to invoke downscaling by enhancing Arc translation through its 3' UTR and causing the subsequent removal of post-synaptic AMPA receptors. Synaptic scaling was occluded when we depleted Trim32 and overexpressed MOV10 in neurons, suggesting that the Trim32-MOV10 axis is necessary for synaptic downscaling. We propose a mechanism that exploits a translation-driven protein degradation paradigm to invoke miRISC remodeling and induce homeostatic scaling during chronic network activity.

24 **Introduction:**

25 Neurons employ a unique strategy, known as synaptic scaling, to counter the run-away
26 excitation and subsequent loss of input specificity that arise due to Hebbian changes; they rely
27 on a compensatory remodeling of synapses throughout the network while maintaining
28 differences in their synaptic weightage [1–6]. Synaptic scaling is achieved by a complex
29 interplay of sensors and effectors within neurons that serve to oppose global fluctuations in a
30 network and establish synaptic homeostasis by modifying post-synaptic glutamatergic currents
31 in a cell-autonomous manner [7–9]. In the context of homeostatic scaling, 'sensors' are
32 classified as molecules that sense deviations in the overall network activity and 'effectors'
33 scale the neuronal output commensurately.

34 Till date not much is known about the repertoire of molecular "sensor" cascades that serve to
35 link events where neurons sense deviations in the network firing rate and subsequently initiate
36 the scaling process. Few molecular sensors have been identified; the eukaryotic elongation
37 factor eEF2 and its dedicated kinase, eEF2 kinase or CamKIII are the two reported thus far
38 [10]. One cascade discovered in this context is the mTORC1 (mammalian Target Of
39 Rapamycin Complex-1) signalling pathway that regulates presynaptic compensation in
40 neurons by promoting BDNF synthesis in the post-synaptic compartment [11,12]. In contrast,
41 AMPA-receptors (AMPARs) have been identified, by overwhelming consensus, to be the
42 predominant "end-point-effectors" in all paradigms of synaptic scaling [13–16]. Unlike
43 NMDARs, AMPARs undergo *de novo* translation during network destabilizations [17] and
44 chronic changes in the post-synaptic response during scaling has been attributed to the
45 abundance of surface AMPARs (GluA1 and GluA2 subunits) [18]. Among the key modifiers of
46 AMPAR expression, miRNAs are known to play pivotal roles in synaptic scaling [19–22]. Relief

47 from translational repression by miRNAs necessitates that mRNAs exit the functional miRISC
48 (microRNA induced silencing complex). This requires miRISC to undergo dynamic changes in
49 its composition [23,24], a cellular phenomenon previously termed as miRISC remodeling [25].
50 However, what remains surprising is our lack of knowledge about how compositional changes
51 within the miRISC are achieved during scaling.

52 The requirement for discrete sets of sensors and effectors is fulfilled within neurons through
53 varied mechanisms including translation and ubiquitin-mediated proteasomal (UPS)
54 degradation. An enhanced degradation of post-synaptic-density (PSD) proteins including
55 GluA1 and GluA2 has been observed in contexts of altered network excitability [26] whereas
56 complete inhibition of UPS activity was shown to occlude synaptic compensation [27]. The
57 integral role of *de novo* translation in synaptic homeostasis was recently highlighted when
58 proteomic analysis of neurons undergoing upscaling and downscaling revealed a remarkable
59 diversity of newly synthesized proteins. Of particular interest was the significant enrichment in
60 the expression of the proteasome core complex during downscaling [28,29]. The demand for
61 the translation of proteasome complexes implies that proteasomes work alongside translation
62 mechanisms during downscaling. Reports documenting the co-localization of ribosomes and
63 the proteasome in neuronal dendrites [30,31] further emphasize the possibility that these two
64 opposing machineries physically interact within the post-synaptic compartment. The
65 remodeling of the proteome through the dynamic regulation of protein biogenesis and
66 degradation has been termed as cellular 'proteostasis' [32]. However, several questions
67 remain unexplored in the context of cellular proteostasis during homeostatic scaling, such as
68 a) what factor establishes the link between translation and protein degradation machineries to
69 shape the proteome during scaling? b) Which process among translation and degradation

70 takes precedence? c) What are the signalling mechanisms that connect events of 'sensing' the
71 bicuculline-mediated hyperactivity and the final down-regulation of surface AMPARs
72 (sAMPARs)?

73 Here, we demonstrate a defined mechanism of synaptic scaling accomplished through an
74 RNA-dependent coordination between translation and proteasome-mediated degradation. We
75 observe that isolated inhibition of either translation or proteasomal activity offsets synaptic
76 homeostasis. Restoration of homeostasis necessitates the combination of both processes. We
77 provide empirical evidence demonstrating that the interaction between translation and protein
78 degradation machineries is direct and RNA dependent. This coordination is achieved when the
79 two apparatuses are tethered to actively translating transcripts linked to miRISC. Synaptic
80 hyperactivity causes an increased abundance of Trim32 and depletion of MOV10 in
81 polysomes; both Trim32 and MOV10 are members of the miRISC. We find that in contexts of
82 chronic hyperactivity, mTORC1-dependent translation of the E3 ligase Trim32 promotes the
83 poly-ubiquitination and subsequent degradation of MOV10 by proteasome. This is triggered by
84 the mTORC1-mediated phosphorylation of its downstream effector, p70 S6 kinase (p70
85 S6K) .We observe that MOV10 degradation leads to enhanced translation of Arc and results in
86 the reduced distribution of sAMPARs. Loss of MOV10 alone is sufficient to decrease the
87 synaptic strength by reducing sAMPARs and mimic events similar to hyperactivity-driven
88 downscaling. Notably, the observed increase in Arc expression in the context of synaptic
89 downscaling happens *via* translation and not by transcriptional mechanisms.

90

91

92 **Results**

93 **Co-dependence of protein synthesis and degradation drives synaptic homeostasis**

94 To test the existence of coordination between translation and degradation in the regulation of
95 synaptic homeostasis, we measured miniature excitatory postsynaptic currents (mEPSCs)
96 from cultured hippocampal neurons (DIV 18-24) after pharmacological inhibition of protein
97 synthesis (anisomycin, 40μM) and proteasomal activity (lactacystin, 10μM) for 24 hours.
98 Application of either lactacystin or anisomycin increased (2.43 ± 0.43 pA, $p<0.02$) and
99 decreased (5.86 ± 0.13 pA, $p<0.01$) mEPSC amplitude respectively. Co-application of both
100 inhibitors restored mEPSC amplitude to that of vehicle treated neurons (Figure 1A-B). The
101 frequency of mEPSCs remained unaltered upon inhibition of translation and proteasome
102 blockade either alone or in combination (Figure 1C), suggesting that this could be a post-
103 synaptic phenomenon. Our data implies that interfering with either protein synthesis or
104 degradation disturbs the balance of synaptic activity, while blocking both synthesis and
105 degradation altogether restores it. Next, we stimulated synaptic downscaling using bicuculline
106 (10μM, 24 hours) and observed that, like previous reports , here too, chronic application of
107 bicuculline lead to a significant decrease in mEPSC amplitude (5.70 ± 0.08 pA, $p<0.01$)
108 without any detectable change in frequency (Figure 1D-F). The extent of decrease in mEPSC
109 amplitude within bicuculline-treated neurons recapitulated the decrease observed in neurons
110 where translation was blocked (bicuculline treated neuron 5.70 ± 0.08 pA decrease *vs.*
111 anisomycin treated neuron 5.86 ± 0.13 pA decrease) (Figure 1B and 1E). We measured the
112 mEPSC amplitude and frequency from hippocampal neurons when bicuculline was co-applied
113 with anisomycin and lactacystin. The dual application of bicuculline and anisomycin did not
114 result in any significant change in mEPSC amplitude when compared to neurons treated with

115 bicuculline alone (Figure 1D-E). This confirms that, rather than inducing an additive effect,
116 chronic inhibition of protein synthesis in itself is sufficient to induce downscaling and could
117 potentially override the effect observed due to bicuculline. Disruption of proteasome function
118 by lactacystin during bicuculline-treatment led to a significant increase in mEPSC amplitude
119 (9.46 ± 0.07 pA increase as compared to bicuculline treated neurons, $p<0.001$) without altering
120 frequency (Figure 1E-F). The increase was effectively more than the basal activity of vehicle-
121 treated neurons (3.76 ± 0.08 pA, $p<0.01$) and mimicked the increase in mEPSC amplitude
122 brought by lactacystin alone (Fig 1B and 1E). Although the influence of lactacystin on mEPSC
123 amplitude is opposite to that of anisomycin, their individual effects override that of bicuculline in
124 each condition. Co-application of both inhibitors during bicuculline-induced hyperactivation
125 produced mEPSC amplitudes comparable to vehicle treated neurons (Figure 1E). Our data
126 indicates that the co-inhibition of translation and degradation restricts any molecular changes
127 away from the basal level, thus, maintaining the synaptic strength at the established
128 physiological set point.

Figure:1

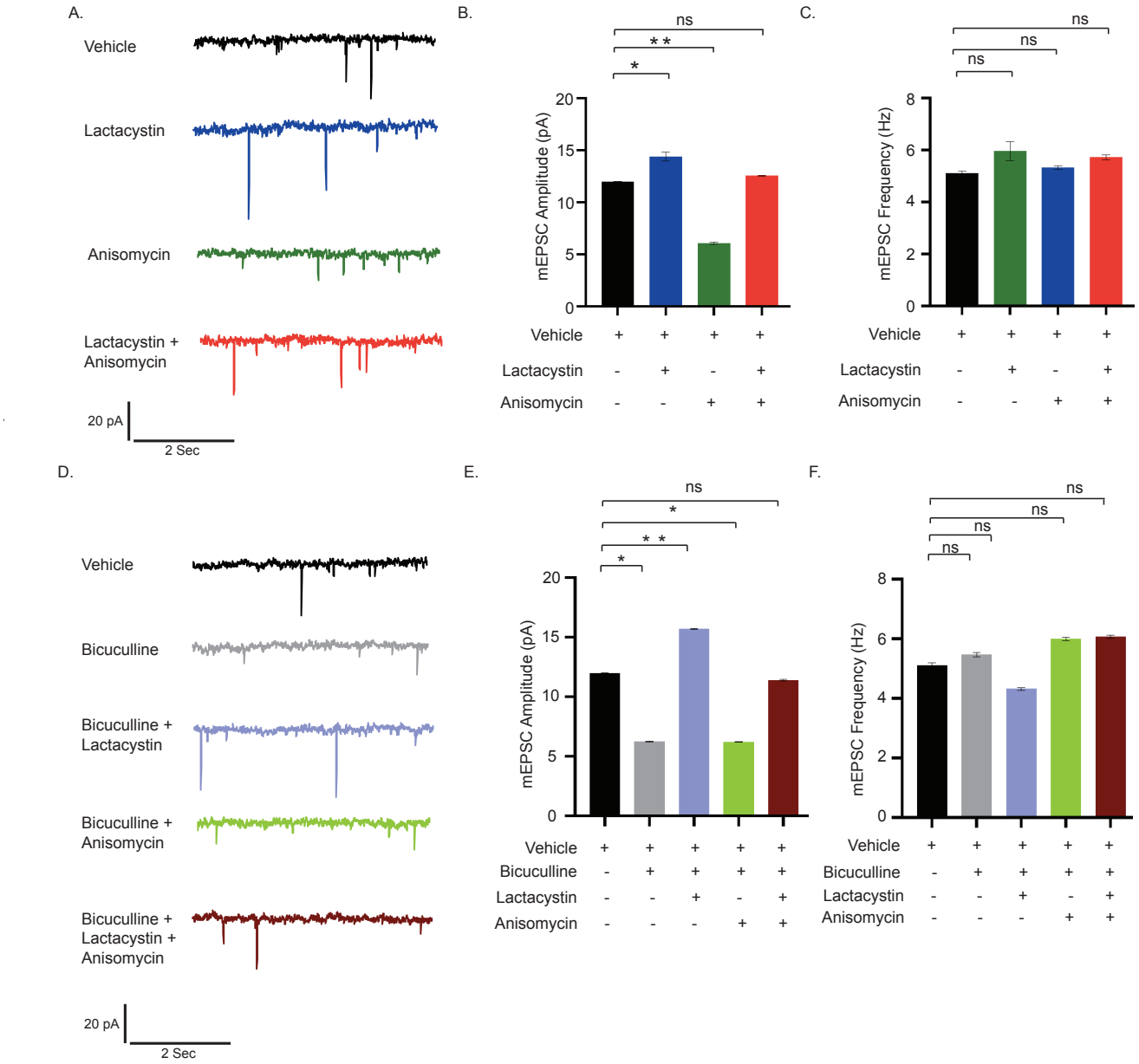

Figure 1: Synaptic scaling is co-regulated by protein synthesis and degradation.

(A-C) mEPSC traces from hippocampal neurons treated with vehicle, lactacystin, anisomycin and both (A). Mean mEPSC amplitude (B) and frequency (C). n=13-15. *p<0.024, **p<0.01. ns, not significant. Data shown as Mean ± SEM. One Way ANOVA and Fisher's LSD. Scale as indicated.

(D-F) mEPSC traces from neurons treated with vehicle, bicuculline alone or in combination with lactacystin, anisomycin (D). Mean mEPSC amplitude (E) and frequency (F). n=12–16. *p<0.01, **p<0.001. ns, not significant. Data shown as Mean ± SEM. One Way ANOVA and Fisher's LSD. Scale as indicated.

138 **Synchronized translation and degradation regulates AMPAR distribution during scaling**

139

140 Since adjustment of synaptic strengths is directly correlated to the surface distribution of
141 surface AMPARs (sAMPARs), we measured the surface expression of GluA1 and GluA2
142 (sGluA1/A2) to identify how concerted mechanisms of synthesis and degradation influence the
143 distribution of sAMPARs during scaling. Neurons (DIV 21-24) were live-labeled using N-
144 terminus specific antibodies against GluA1 and GluA2 following bicuculline treatment, either
145 alone or in presence of both anisomycin and lactacystin, for 24 hours and synapses marked by
146 PSD95. The surface expression of sGluA1/A2 in excitatory neurons was decreased following
147 network hyperactivity (50.6 ± 6.68%, $p<0.01$ for sGluA1 and 26.1 ± 6.62%, $p<0.01$ for sGluA2)
148 (Figure 2A-D, S1 A-B). Consistent with our electrophysiological data, inhibition of both the
149 translation and the proteasome in bicuculline-treated neurons increased sGluA1/A2 levels
150 (133.95 ± 8.77 %, $p<0.01$ for sGluA1, 53.17 ± 6.44%, $p<0.001$ for sGluA2) when compared to
151 neurons treated with bicuculline alone (Figure 2C-D, S1A-B). Thus our data indicates that a
152 dual inhibition of protein synthesis and degradation restores the synaptic sGluA1/A2 following
153 network hyperactivity.
154 To reaffirm whether AMPARs are indeed the end-point effectors of synaptic downscaling, we
155 used $GluA2_{3Y}$, a synthetic peptide derived from the GluA2 carboxy tail of AMPA receptors to
156 block the endocytosis of the AMPARs [13], effectively ensuring that the number of AMPARs
157 remain unchanged throughout 24 hours. Consistent with previous studies, no significant
158 changes in mEPSC amplitude were detected upon inhibition of GluA2 endocytosis during
159 chronic application of bicuculline ($GluA2_{3Y}$ treated neuron 11.01 ± 0.36 pA *vs.* $GluA2_{3Y}$ +
160 bicuculline treated neuron 12.17 ± 0.28 pA, $p<0.49$) (Figure 2E-F).

Figure: 2

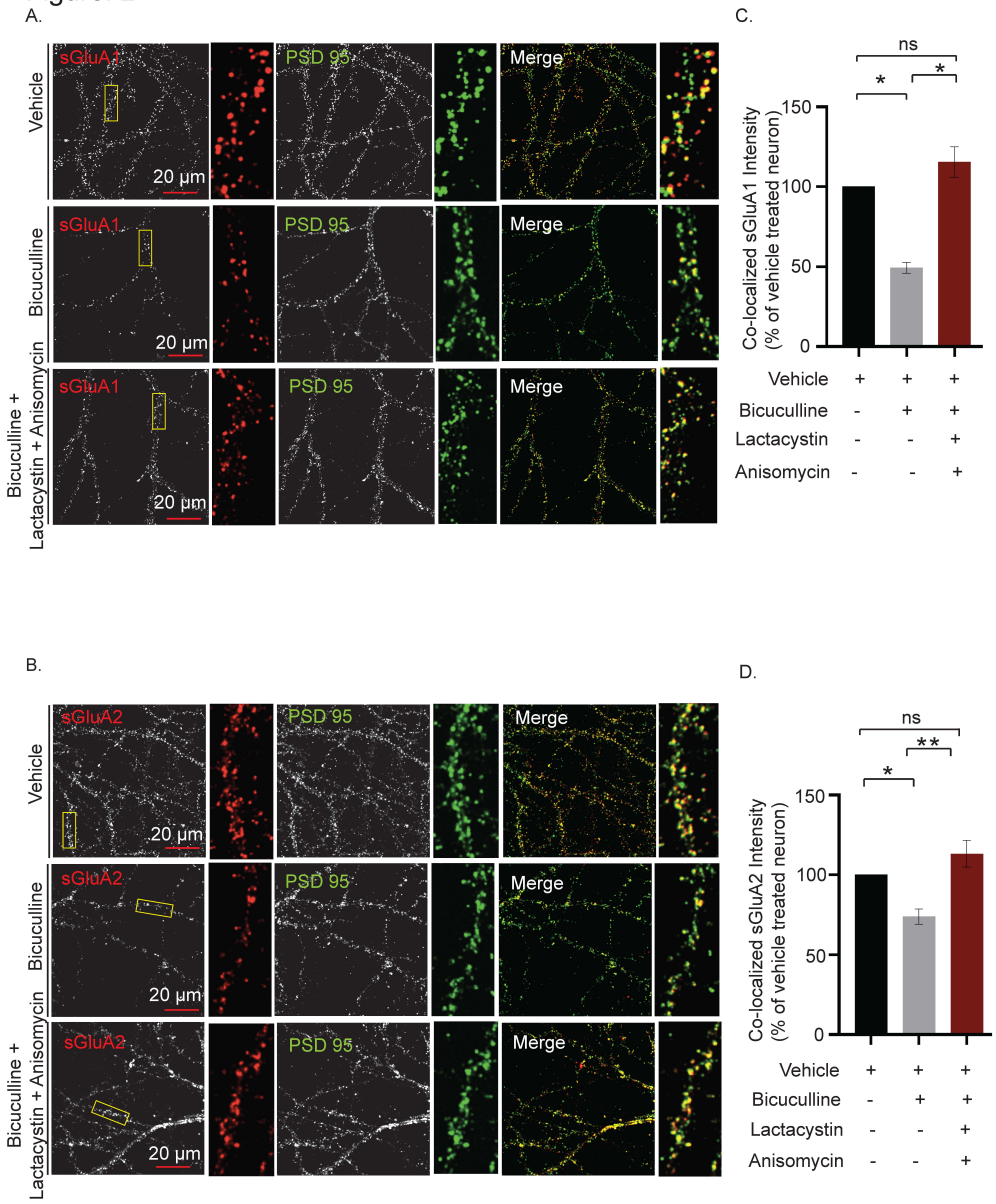
A.
Vehicle
Bicuculline
Bicuculline + Lactacystin + Anisomycin
sGluA1
PSD 95
Merge
20 µm
C.
ns
*
*
Co-localized sGluA1 Intensity (% of vehicle treated neuron)
150
100
50
0
Vehicle + + +
Bicuculline - + +
Lactacystin - - +
Anisomycin - - +
B.
sGluA2
D.
**
Co-localized sGluA2 Intensity (% of vehicle treated neuron)

161

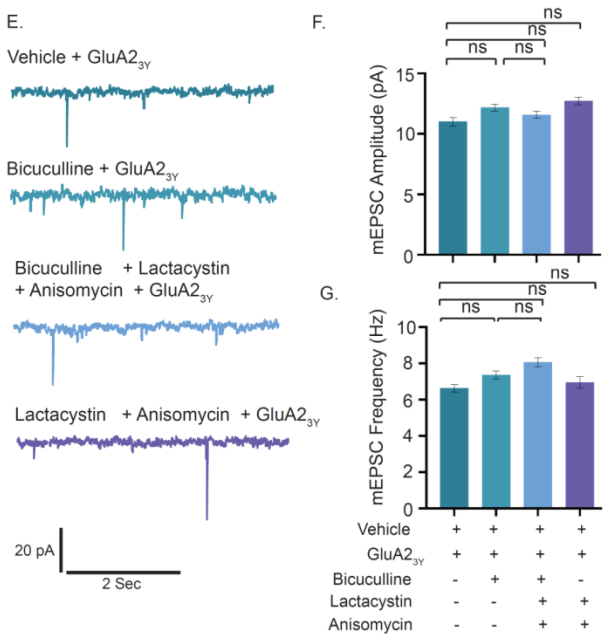

Figure 2: Co-inhibition of protein synthesis and degradation restores hyperactivity driven reduction of synaptic AMPAR expression

(A-D) High magnification images of sGluA1 or sGluA2 (red), PSD95 (green) and sGluA1/PSD95 (A) or sGluA2/PSD95 (B) (merged) images from neurons treated with vehicle, bicuculline alone or in combination with lactacystin and anisomycin. Normalized intensity of sGluA1 (C) or sGluA2 (D) co-localized with PSD95 particles. n=56-57, sGluA1 and n=31-63, sGluA2. *p<0.01, **p<0.001. One Way ANOVA and Fisher's LSD. Dendrite marked in yellow box was digitally amplified.

(E-G) mEPSCs traces from hippocampal neurons treated with $GluA_{23y}$ either alone or in presence of bicuculline, lactacystin + anisomycin and bicuculline + lactacystin + anisomycin (E). Mean mEPSC amplitude (F) and frequency (G). n=10 - 13. ns, not significant. Data is shown as Mean ± SEM. One Way ANOVA and Fisher's LSD. Scale as indicated. See also Figure S1.

Application of GluA2$_{3Y}$ did not alter mEPSC amplitude as compared to vehicle treated neurons (GluA2$_{3Y}$ treated neuron 11.01 ± 0.36 *vs.* vehicle treated neurons 11.94 ± 0.07 pA) (Figure S1C-D), nor any change observed between neurons treated with GluA2$_{3Y}$ and those treated with both lactacystin and anisomycin in presence or absence of bicuculline (Figure 2F-G). mEPSC frequency remained unaltered throughout while mEPSC amplitude in each condition

182 was similar to that of control neurons (Figure 2G, S1E). Collectively, these observations
183 indicate that changes in the abundance of surface-AMPARs during scaling is facilitated by
184 proteomic remodeling that exploits both translation and degradation processes.
185
186 **RNA-dependent co-sedimentation of the proteasome and translation regulators**
187
188 The co-localization of polyribosomes and proteasomes to sites of synaptic activity [30,31] lead
189 us to examine whether the components of the 26S proteasomal machinery could remain
190 physically associated with actively translating transcripts in order to make the necessary
191 proteomic changes. These components include proteins forming the 19S regulatory subunits
192 and the 20S proteasome core. We analyzed polysomes from the hippocampus of 8-10 week
193 old rats and assessed whether the sedimentation pattern of proteasomes matches those of
194 actively translating, polyribosome-associated mRNA fractions. We observed that several
195 components of the proteasomal machinery such as α7 subunit of the 20S proteasome; and
196 Rpt1, Rpt3 and Rpt6 subunits of the 19S proteasome co-sedimented with translation initiation
197 factors such as eIF4E and p70S6 kinase within actively translating polysomes (Figure 3A-B,
198 S2A). We also detected the polysomal distribution of MOV10, a helicase and an RNA binding
199 protein known to be poly-ubiquitinated upon synaptic activation, and Trim32, an E3 ligase, both
200 components of the miRISC [33] (Figure 3A-B).
201 RNAse or EDTA treatment of cytoplasmic lysates prior to density gradient fractionation led to a
202 complete collapse of the polysome profile, simultaneously shifting the sedimentation of Rpt6,
203 Rpt1, α7, eIF4E, MOV10, Trim32 to the lighter fractions (Figure 3C-F, S2B-C). The disruption
204 of association between the translational and proteasomal components on RNase and EDTA

205 treatment suggests that translating transcripts are necessary to recruit the translation and
206 proteasome machineries. These observations ruled out the possibility that the observed co-
207 sedimentation was a result of similar densities between the protein complexes and polysomes.
208 Trim32 and MOV10 in specific high-density sucrose fractions (fraction # 8/11/15) were not
209 detected due to loss of proteins during the TCA precipitation step (Figure 3B). Furthermore, we
210 saw that the polysome-associated 26S proteasome is catalytically active as detected by its
211 ability to cleave a fluorogenic proteasome substrate that is blocked by the proteasome inhibitor
212 epoxymycin (Figure 3G-H, S2D).

Figure:3

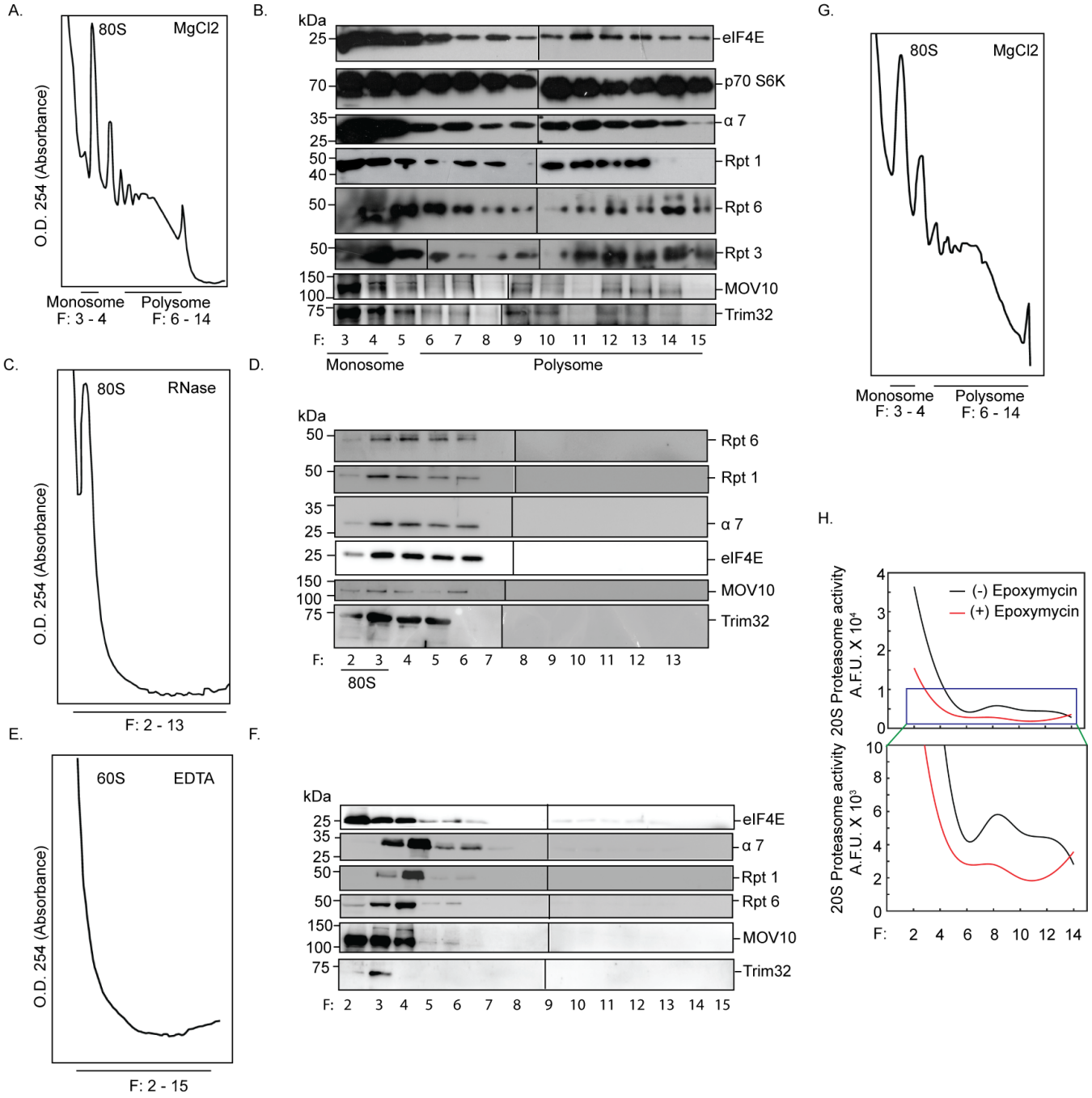

Figure 3: RNA-dependent association between active proteasomes and translating polyribosomes

(A-F) Absorbance profile at 254nm (A_{254}) of fractionated cytoplasmic extracts from hippocampal tissue incubated without (A) or with RNase (C) or with EDTA (E). Monosome (80S) or 60S Ribosome or Polysome fractions as indicated. Western blot analysis of fractions without (B) or with RNase (D) or with EDTA (F) treatment showing

219 distribution of translation regulators eIF4E and p70S6 Kinase; α7 subunit of 20S core and Rpt1, Rpt3, Rpt6 of 19S
220 cap; miRISC proteins MOV10 and Trim32.
221 (G-H) A_{254} profile of fractionated cytoplasmic extract (G) and quantitation of catalytic activity of proteasomes
222 present in alternate fractions from two polysome preparations (H). See also Figure S2.
223

224 **Proteasome and the regulators of translation directly interact with each other within**
225 **excitatory neurons.**

226 Whole-cell patch clamp recordings from hippocampal excitatory neurons demonstrated that the
227 co-regulation of translation and proteasome-mediated protein degradation is necessary for
228 synaptic homeostasis. Consistent with this observation, co-sedimentation of proteasome
229 subunits along with polysomes linked to protein synthesis regulators and members of the
230 miRISC led us to enquire whether components of the ternary complex directly interact with
231 each other in excitatory neurons of the hippocampus. To evaluate this; we immunoprecipitated
232 the 19S proteasomal complex using Rpt6 antibody from hippocampal neurons. We observed
233 the co-precipitation of eEF2, a translation elongation factor that functions as a “sensor” of
234 change in network activity (Figure 4A). We also found that a known regulator of the mTORC1-
235 dependent protein synthesis; p70 S6 kinase as well as its phosphorylated form [34] co-
236 precipitated with the 19S proteasome (Figure 4A). We further analyzed the proteins interacting
237 with polysomes within excitatory neurons by expressing haemagglutinin (HA)-tagged ribosomal
238 protein Rpl22 (HA-Rpl22) that gets incorporated into polysomes [35,36] (Figures 4B-D, S2E).
239 We reasoned that the analysis of HA-Rpl22-affinity purified complexes would confirm whether
240 the polysome-associated translation and degradation machineries directly interact with each
241 other.

Figure: 4

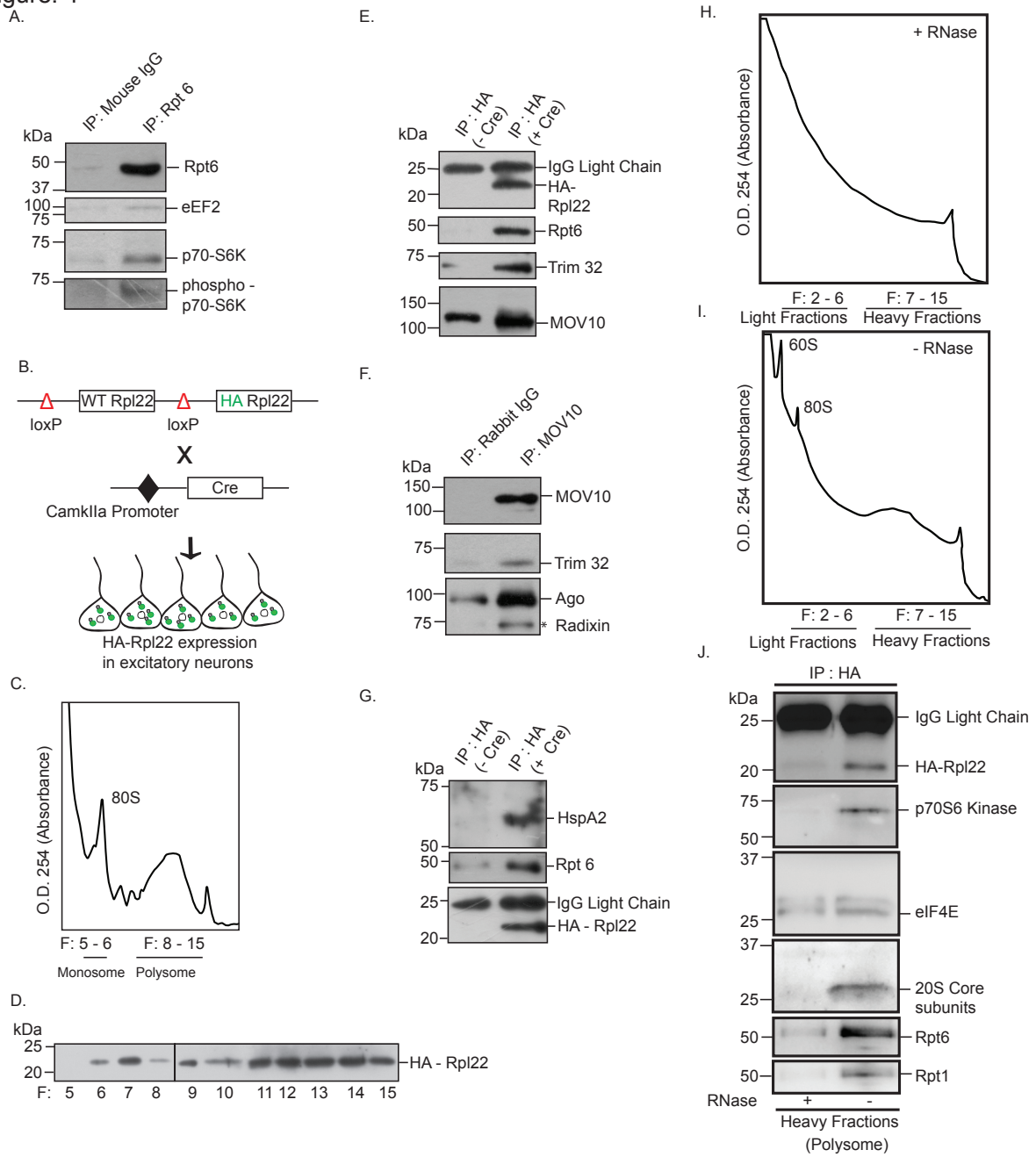

242

243 **Figure 4: Interaction between proteasome and actively translating RNA-associated polyribosomes.**

244 (A) Proteasome associated protein complex was immunoprecipitated from hippocampal lysate using antibody
245 against Rpt6 and mouse IgG. Western blot of purified protein complex performed using antibodies against eEF2,
246 p70S6 Kinase, phospho-p70S6 kinase. (B) RiboTag mouse crossed with CamKIIa promoter-driven Cre
247 recombinase mouse results in deletion of wild-type Rpl22 ribosomal protein and replacement of HA tagged Rpl22
248 in forebrain excitatory neurons.

(C) A_{254} profile showing indicated fractions of Monosome and Polysome. (D) Polysome fractions showing enrichment of HA-Rpl22 as detected by western blot using antibody against HA. (E) HA-tagged Rpl22 containing polyribosome affinity purified using antibody against HA. Western blot analysis of affinity purified complex using antibodies against HA, Rpt6, Trim32 and MOV10.

(F) MOV10 was immunoprecipitated from hippocampal lysate. Western blot analysis of MOV10-immunoprecipitated protein complex showed the co-precipitation of Trim32 with miRISC components MOV10 and Ago.

(G) Detection of HspA2 and Rpt6 in HA affinity purified protein complex from HA-Rpl22 expressing neurons by western blot using antibody against HspA2 and Rpt6 and HA.

(H – I) A_{254} profile showing indicated fractions of Monosome and Polysome obtained from cytoplasmic lysates treated with (H) or without (I) RNase prior to density gradient fractionation.

(J) HA-tagged Rpl22 containing ribosomes affinity purified from heavy fractions of sucrose gradient using antibody against HA. Western blot analysis of affinity purified complex using antibodies against HA, p70 S6 kinase, eIF4E, 20S Core subunits, Rpt6 and Rpt1.

Our western blot analysis of HA-Rpl22 affinity-purified protein complex showed that Rpt6 directly interacts with Trim32 and MOV10 (Figure 4E). Immunoprecipitation of MOV10 from hippocampal neurons resulted in the co-precipitation of both Argonaute (Ago) and Trim32, confirming that the latter is an integral component of the Ago-containing miRISC (Figure 4F). We also detected the chaperone protein HspA2 in the HA-affinity purified fraction along with Rpt6 (Figure 4G), suggesting that HspA2 could tether proteasomes to actively translating transcripts. The direct interaction between components of the translation and proteasome machinery could occur without the participation of polysome-associated, translating mRNA. To evaluate whether the observed association was RNA-dependent or RNA-independent, HA-Rpl22-affinity purified protein complexes from polysome fractions of hippocampal tissue lysates treated with or without RNase were analyzed. Our western blot analysis revealed that the 20S proteasome core, Rpt6 and Rpt1 co-precipitated with eIF4E and p70 S6 kinase (Figure 4J). RNase treatment of the cytoplasmic lysate prior to density gradient fractionations prevented this interaction on the actively translating, heavier fractions of the polysome (Figure

278 4J). This demonstrates that polysome-associated, translating RNA act as scaffolds to facilitate
279 the direct interaction between protein synthesis and degradation modules.
280
281 **Chronic hyperactivity in neurons regulates the distribution of factors associated with**
282 **translation and the proteasomal machinery**
283 Once we identified that members of the translation apparatus, the 26S proteasome and the
284 miRISC remain directly associated on polysomes, we investigated the effect of prolonged
285 neuronal hyperactivity on the polysomal distribution of these factors in the context of synaptic
286 homeostasis. To evaluate the hyperactivity-regulated polysome association, density gradient
287 fractions from neurons treated with either bicuculline (10μM, 24 hours) or vehicle were
288 analyzed by western blot using antibodies against translation regulators, proteasome subunits,
289 chaperone and members of the miRISC. We observed a relative enrichment of the translation
290 elongation factor eEF2, mTORC1 downstream effector p70 S6 kinase as well as its
291 phosphorylated form and the phosphorylated ribosomal protein S6 in polysome fractions
292 following prolonged neuronal activity (Figure 5A - D). Similar to enrichment of translation
293 regulators, we also observed an enrichment of 20S core proteasome subunits upon bicuculline
294 treatment (Figure 5A – D). The chaperone protein HspA2 was detected in polysome fractions
295 in both vehicle-treated and bicuculline-treated neurons (Figure 5A – D). The core component
296 of the miRISC, Argonaute showed a relative depletion from polysome fractions in bicuculline-
297 treated neurons as compared to vehicle-treated neurons. Furthermore, we observed that the
298 abundance of Trim32 was enhanced (108.3 ± 7.74% increase, $p<0.005$) whereas MOV10
299 (72.37 ± 3.54% decrease, $p<0.002$) was depleted from polysome in response to synaptic
300 hyperactivity (Figure 5 C –F).

Figure 5

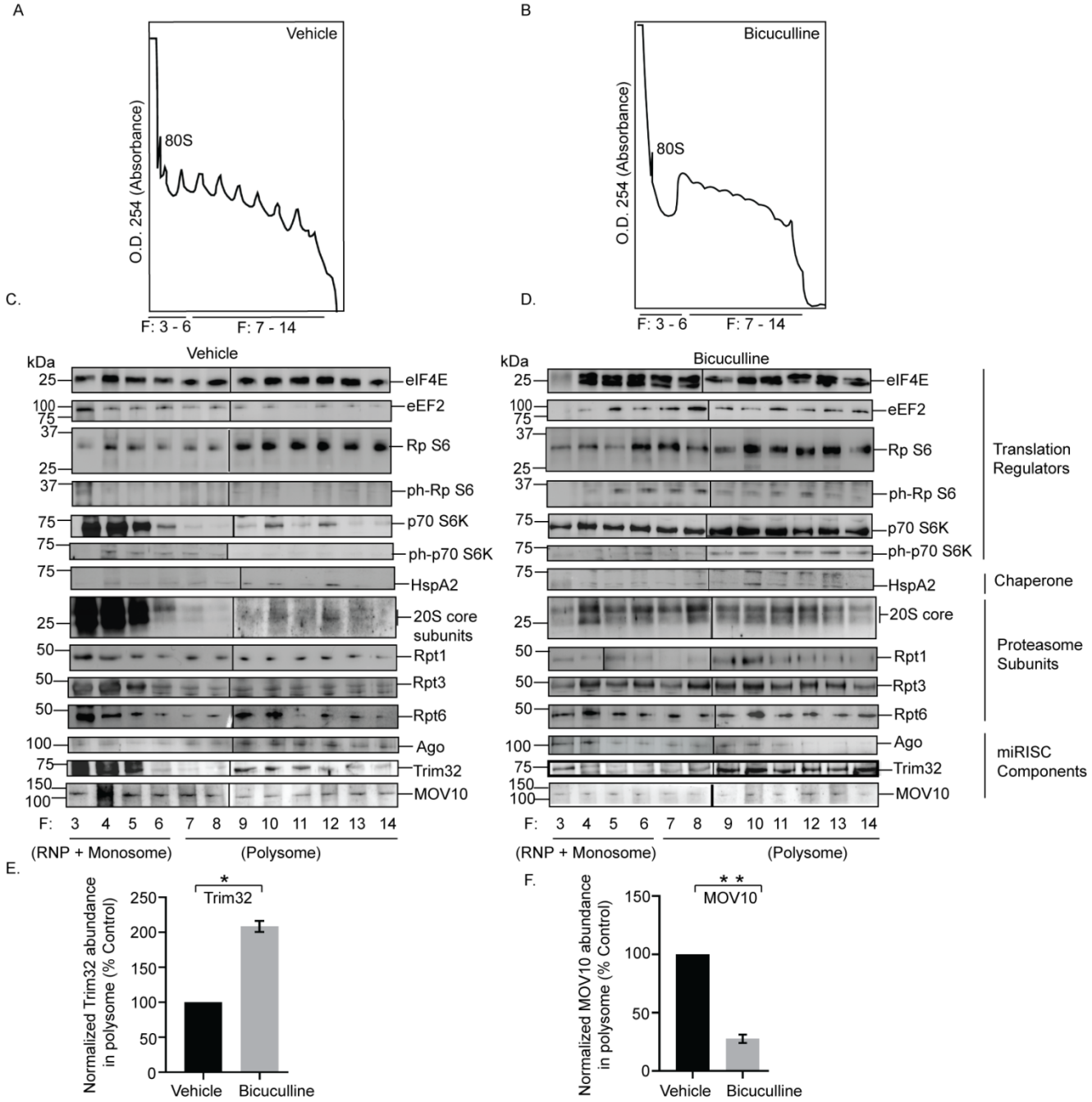

Figure 5: Hyperactivity-dependent polysome distribution of proteasome, translation regulators and component of miRISC.

(A-B) Absorbance profile at 254nm (A_{254}) of fractionated cytoplasmic extracts from cortical neurons treated with vehicle (A) or bicuculline (B). Monosome (80S) or Polysome fractions as indicated. Western blot analysis of fractions from vehicle (C) or bicuculline (D) treated neurons showing distribution of translation regulators eIF4E,

308 eEF2, ribosomal protein S6 (Rp S6), phosphorylated ribosomal protein S6 (ph-Rp-S6), p70 S6 Kinase (p70 S6K),
309 phosphorylated p70 S6 Kinase (ph-p70 S6K); chaperone protein HspA2; proteasome subunit of 20S core and
310 Rpt1, Rpt3, Rpt6 of 19S cap; miRISC proteins Argonaute (Ago), MOV10 and Trim32. (E) Quantitation of
311 polysome distribution of Trim32. (F) Quantitation of polysome distribution of MOV10. *p<0.005, **p<0.002. n=3,
312 Unpaired t-test with Welch's correction. RNP: Ribonucleoprotein. See also Figure S2.
313

---

314 Comprehensively, these data point toward activity-induced dynamicity in polysome association
315 of factors regulating synaptic homeostasis.
316

317 **Translation drives proteasomal degradation to cause miRISC remodeling during**
318 **synaptic downscaling**
319

320 The reciprocal pattern of abundance of MOV10 and Trim32 in polysomes upon chronic
321 hyperactivity (Figure 5E-F) and their association with Argonaute (Figure 4F), a core member of
322 the miRISC, prompted us to analyze their expression in the context of synaptic downscaling.
323 Bicuculline treatment of hippocampal neurons (DIV 18 - 21) enhanced (108.2 ± 7.55%
324 increase, p<0.0001) Trim32 with a concomitant decrease (65.94 ± 2.67% decrease, p<0.001)
325 in MOV10 (Figure 6A-C). The increase in Trim32 expression post bicuculline treatment was
326 blocked by anisomycin and surprisingly resulted in the inhibition of MOV10 degradation
327 (184.82 ± 10.77% protected MOV10, p<0.03) (Figure 6C). This indicates that the degradation
328 of MOV10 is dependent on enhanced Trim32 synthesis and that Trim32 translation precedes
329 the commencement of MOV10 degradation. Treatment with lactacystin resulted in the
330 expected protection of MOV10 from degradation (202.41 ± 3.18% MOV10 protected, p<0.006)
331 upon bicuculline-induced hyperactivity (Figure 6C); whereas there remained no change in the
332 Trim32 expression levels (Figure 6B). Co-application of lactacystin and anisomycin during
333 bicuculline-induced hyperactivity changed the expression of MOV10 and Trim32

334 commensurate to basal levels (Figure 6B-C). We did not observe any alteration of Argonaute
335 expression upon prolonged bicuculline treatment of hippocampal neurons (Figure S3A-B).
336 Chronic inhibition of protein synthesis alone, without bicuculline treatment, led to a modest but
337 statistically significant decrease of both Trim32 (22.42 ± 0.70% decrease, $p<0.001$) and
338 MOV10 (28.14 ± 0.48% decrease, $p<0.0003$) (Figure S3C-E), whereas chronic inhibition of the
339 proteasome alone has no effect on Trim32 and MOV10 expression (Figure S3C-E) under
340 basal conditions. The significant decrease of both proteins upon anisomycin treatment may be
341 due to the combined effect of global inhibition of translation and the on-going basal level of
342 protein degradation.
343 The observed reciprocity between MOV10 and Trim32 expression levels on chronic bicuculline
344 treatment led us to analyze whether Trim32 is the sole E3-ligase responsible for the UPS-
345 mediated degradation of MOV10. Knockdown of Trim32 prevented the bicuculline-induced
346 degradation of MOV10 (199.41 ± 0.69% protected, $p<0.0001$) (Figure 6D-E). Moreover, loss of
347 Trim32 alone enhanced the expression of MOV10 (58.3 ± 3.09% increase, $p<0.0001$) as
348 compared to basal level (Figure 6D-E). We immunoprecipitated MOV10 from bicuculline or
349 vehicle treated hippocampal neurons expressing shRNA against Trim32 or control shRNA.
350 MOV10 ubiquitination was analyzed by western blot using an antibody that specifically
351 recognizes polyubiquitin conjugates. We observed that bicuculline-induced polyubiquitination
352 of MOV10 was abrogated by Trim32 knockdown (Figure 6F). These observations indicate that
353 a) the translation of Trim32 is a prerequisite for the degradation of MOV10 by proteasome
354 during synaptic downscaling and b) Trim32 is the only E3 ligase necessary and sufficient for
355 MOV10 ubiquitination.

Figure: 6

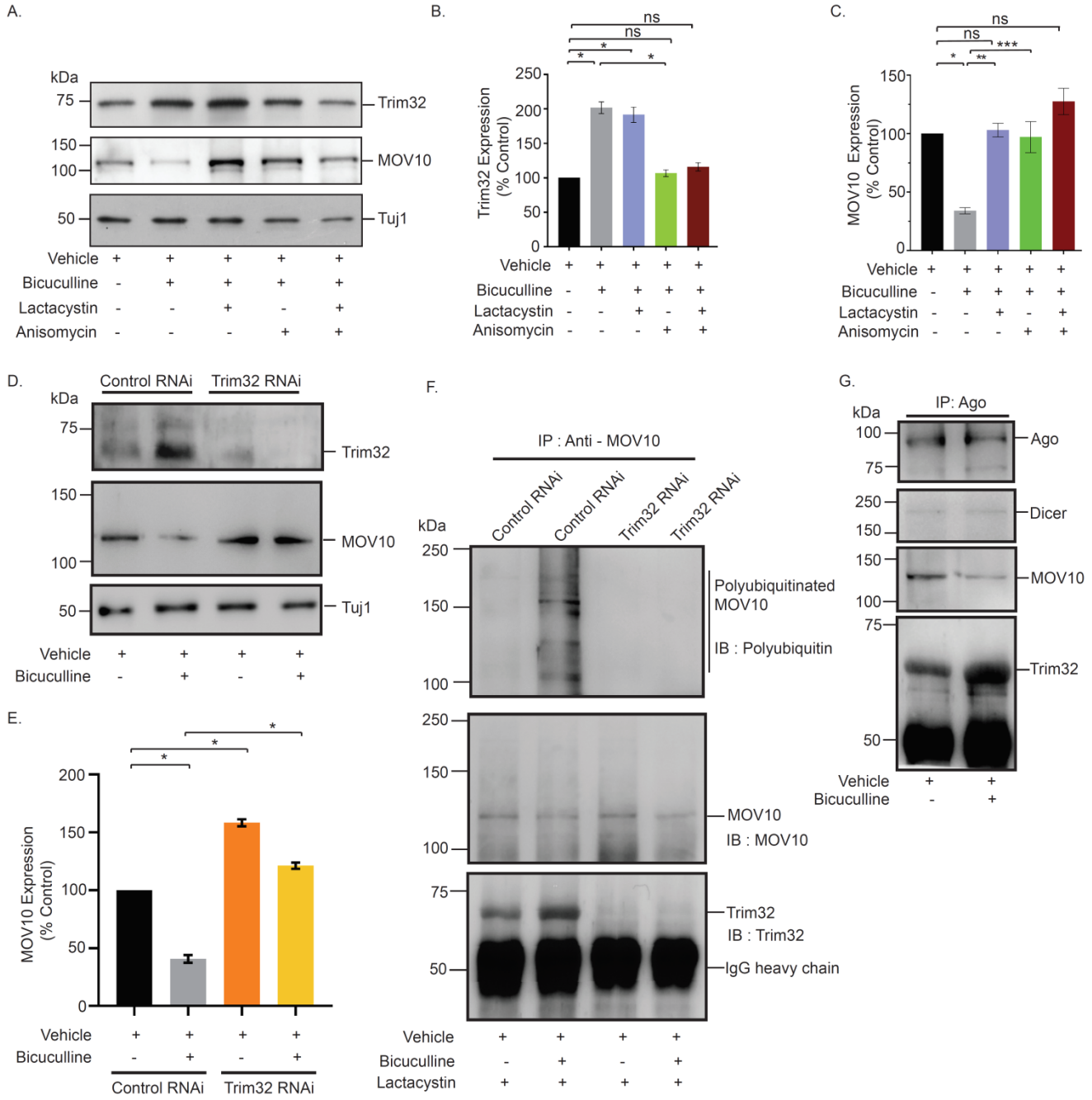

Figure 6: Synthesis of Trim32 facilitates polyubiquitination and subsequent degradation of MOV10 for miRISC remodeling.

(A-C) Western blot analysis showing the expression of Trim32, MOV10 and Tuj1 from neurons treated with bicuculline with or without lactacystin, anisomycin or both (A). Quantitation of Trim32 (B) and MOV10 (C) expression. n=3. Data shown as Mean ± SEM. *p<0.0001 (B) and *p<0.001, **p<0.006, ***p<0.02 (C). ns, not significant. One Way ANOVA and Fisher's LSD.

364

365 (D-E) Western blot analysis of bicuculline or vehicle treated neurons infected with lentivirus expressing Trim32 or
366 non-targetting control shRNA showing expression of Trim32, MOV10 and Tuj1 (D). Quantitation of Trim32 (n=5)
367 (E). Data shown as Mean ± SEM. *p<0.0001. Unpaired t-test with Welch's correction.
368

369 (F) MOV10 was immunoprecipitated from hippocampal neurons treated with bicuculline or vehicle in presence of
370 lactacystin. Polyubiquitination of MOV10 was detected by western blot analysis using an antibody against
371 polyubiquitin conjugates (FK1). Western blot analysis of MOV10-immunoprecipitated protein complex showed the
372 co-precipitation of Trim32 in presence or absence of bicuculline.
373

374 (G) Argonaute (Ago) was immunoprecipitated from hippocampal neurons treated with bicuculline or vehicle.
375 Western blot analysis of immunoprecipitated Argonaute complex showed the co-precipitation of miRISC proteins
376 Dicer, MOV10 and Trim32.
377

---

378 Bicuculline-induced changes in Trim32 and MOV10 levels without any change in Argonaute
379 suggest that during synaptic hyperactivity, miRISC remodeling could occur due to Trim32-
380 translation-dependent MOV10 degradation. To confirm this, we have immunoprecipitated
381 Argonaute and analyzed the association of key components of the miRISC post bicuculline
382 treatment for 24 hours. We found a relative depletion of MOV10 and enrichment of Trim32
383 within the silencing complex upon synaptic hyperactivity (Figure 6G). However, the association
384 of Dicer, another member of the miRISC, remains unaffected (Figure 6G). Comprehensively,
385 our data point towards chronic network hyperactivity-induced miRISC remodeling that alters
386 the expression of miRISC members, Trim32 and MOV10.
387

388 **Translation of Trim32 during chronic hyperactivity is mTORC1 dependent**
389

390 Co-precipitation of the downstream effectors of the mTORC1 signaling cascade with the 26S
391 proteosomal subunit Rpt6 (Fig 4A) and the activity-dependent differential distribution of these
392 effectors in polysome (Fig 5C-D) led us to examine whether mTORC1 signaling plays a role

393 in causing synaptic downscaling in response to chronic hyperactivity. Bicuculline-treatment of
394 hippocampal neurons in the presence of rapamycin (100nM, 24 hours), a selective inhibitor of
395 mTORC1, completely abolished the chronic hyperactivity-driven Trim32 synthesis (16.48 ±
396 10.33% increase as compared to control, p=0.45) and consecutive MOV10 degradation (8.19 ±
397 2.81% decrease as compared to control, p=0.06) (Figure 7A-C). Rapamycin treatment alone
398 did not alter the expression patterns of Trim32 and MOV10 (Figure 7A-C). This led us to
399 hypothesize that mTORC1 pathway acts upstream of Trim32, serving to regulate its synthesis
400 in response to chronic bicuculline treatment. Consistent with our biochemical data, we
401 observed that co-incubation of rapamycin and bicuculline prevented the decrease in mEPSC
402 amplitude (2.76 ± 0.13 pA increase as compared to bicuculline treated neurons, p<0.01) but
403 not frequency (Figure 7D-F). Just as above, rapamycin treatment alone has no effect,
404 indicating that chronic hyperactivity acts as a triggering point for mTORC1 activation (Figure
405 7D-F) and this subsequently plays a role in driving Trim32 translation.
406 mTORC1-mediated translation is regulated by the phosphorylation of two divergent
407 downstream effectors, eukaryotic translation initiation factor 4E-binding protein 2 (4EBP-2) and
408 p70 S6 Kinase (p70 S6K) [37]. We examined the phosphorylation status of these two
409 downstream effectors following bicuculline-induced hyperactivity. Chronic bicuculline treatment
410 leads to a significant enhancement of p70 S6 kinase phosphorylation (74.66 ± 2.61 %
411 increase, p<0.0001) which was blocked by rapamycin (Figure 7G-H). However, bicuculline
412 treatment did not affect the phosphorylation of 4EBP2 (Figure 7G and 7I).

Figure: 7

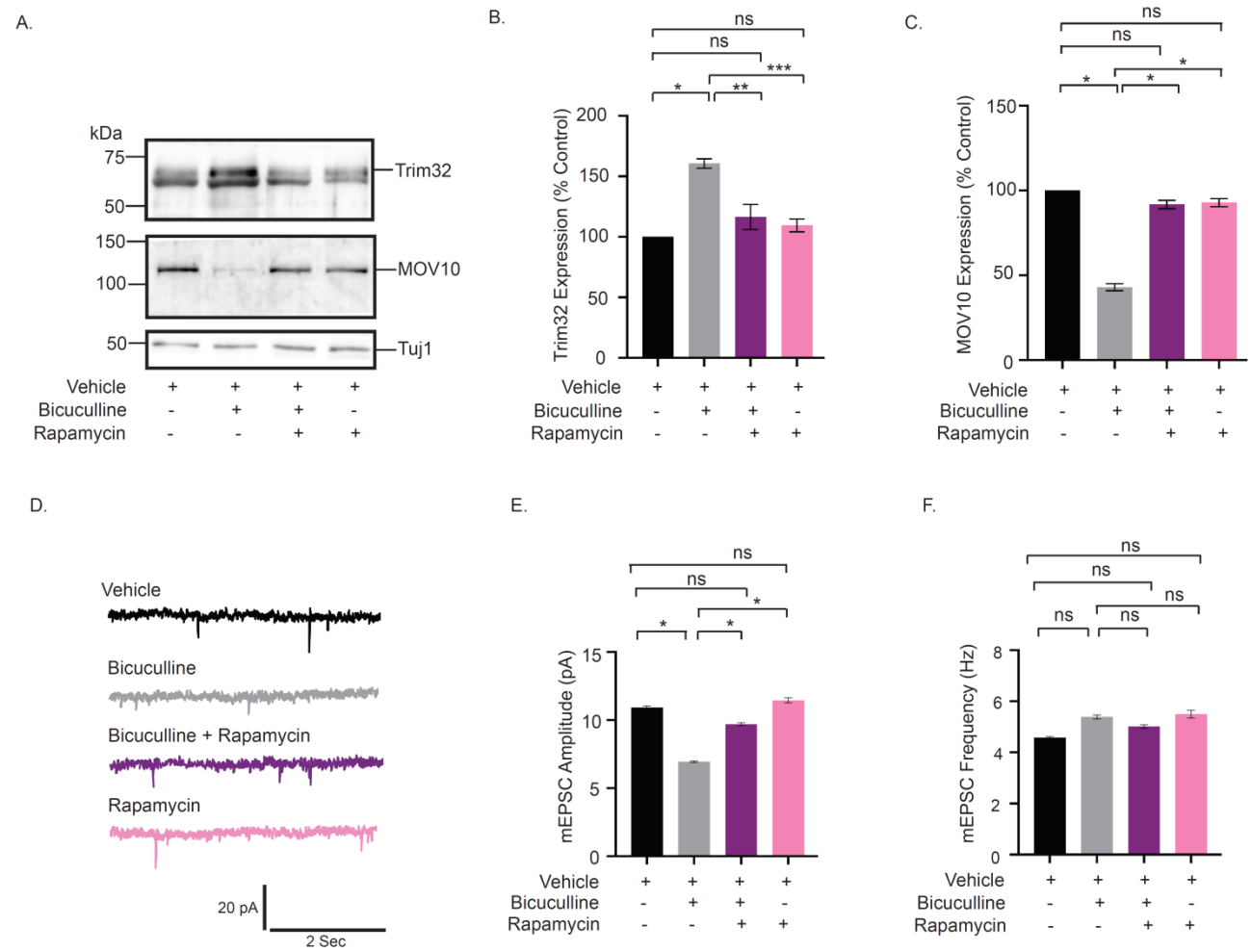
A.
kDa
75
50
150
100
50
Trim32
MOV10
Tuj1
Vehicle + + + +
Bicuculline - + + -
Rapamycin - - + +
B.
Trim32 Expression (% Control)
200
150
100
50
0
ns
ns
***
*
**
C.
MOV10 Expression (% Control)
150
100
50
0
ns
ns
*
*
*
D.
Vehicle
Bicuculline
Bicuculline + Rapamycin
Rapamycin
20 pA
2 Sec
E.
mEPSC Amplitude (pA)
15
10
5
0
ns
ns
*
*
*
F.
mEPSC Frequency (Hz)
8
6
4
2
0
ns
ns
ns
ns
ns

413

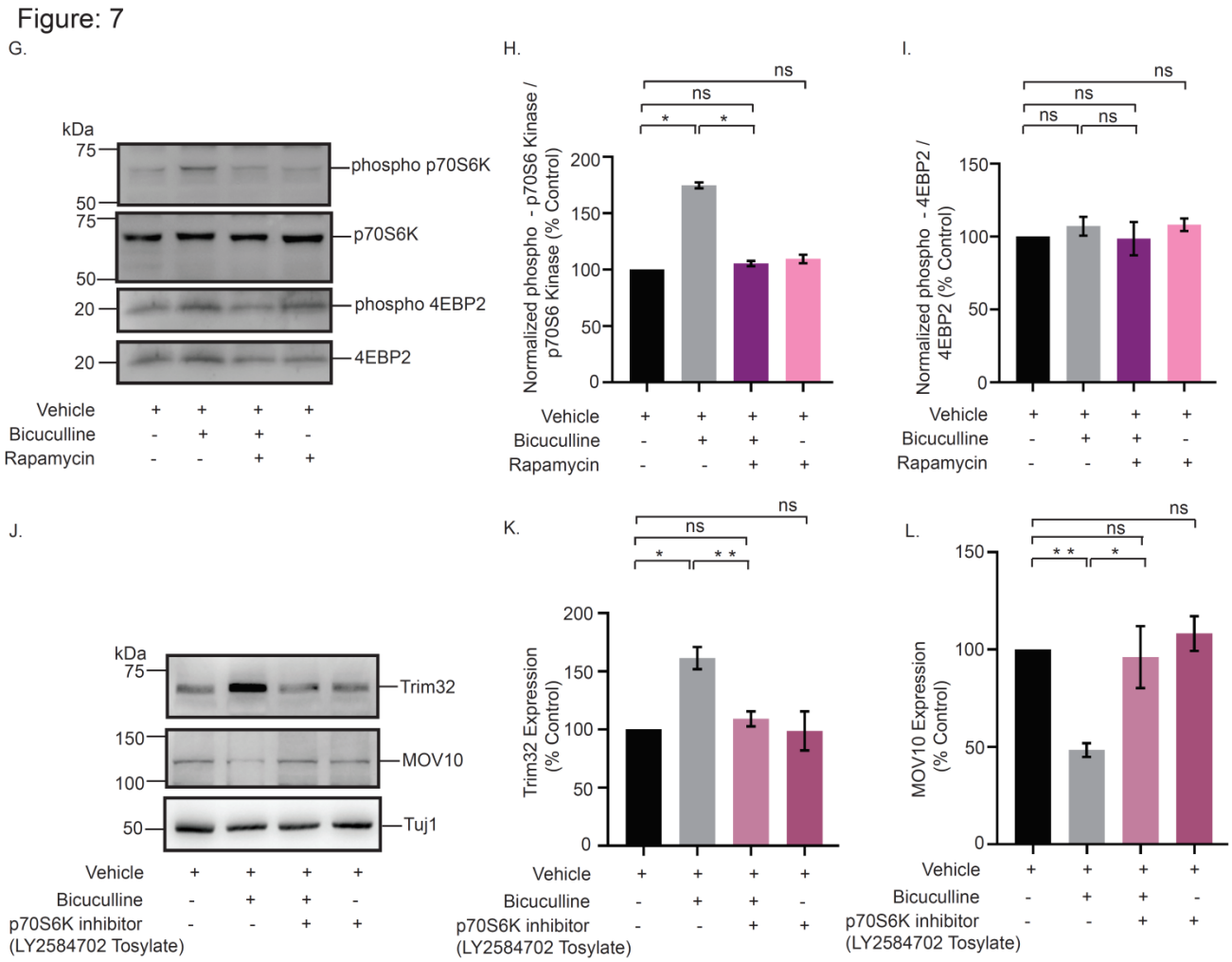

Figure 7: mTORC1 regulates Trim32 synthesis and consequent MOV10 degradation during synaptic downscaling

(A-C) Western blot analysis from neurons treated with bicuculline, rapamycin or both showing expression levels of Trim32, MOV10 and Tuj1 (A). Quantitation of Trim32 (B) MOV10 (C) expression. Data shown as Mean ± SEM. n=5. *p<0.0001, **p<0.0007, ***p<0.0001 (B) and *p<0.001 (C). ns, not significant. One Way ANOVA and Bonferroni's correction.

(D-F) mEPSC traces from neurons treated with vehicle, bicuculline, rapamycin or both (D). Mean mEPSC amplitude (E) and frequency (F). n=8-9. *p<0.01. ns, not significant. Data shown as Mean ± SEM. One Way ANOVA and Fisher's LSD.

(G-I) Western blot analysis from neurons treated with bicuculline, rapamycin or both showing phosphorylation and total expression of p70 S6 Kinase and 4EBP2 (G). Quantitation of p70 S6 Kinase phosphorylation (H) 4EBP2

428 phosphorylation (I). n=4. *p<0.0001. ns, not significant. Data shown as Mean ± SEM. One Way ANOVA and
429 Fisher's LSD.
430
431 (J-L) Western blot analysis from neurons treated with bicuculline, p70 S6 kinase inhibitor LY2584702 Tosylate or
432 both showing expression of MOV10 and Trim32 (J). Quantitation of Trim32 (K) and MOV10 (L). n=5. *p<0.003,
433 **p<0.0002 (K) **p<0.0001, *p<0.02 (L). ns, not significant. Data shown as Mean ± SEM. One Way ANOVA and
434 Fisher's LSD.

435

436 We used a specific inhibitor of p70 S6K, LY2584702 Tosylate (2 μM, 24 hours), in primary
437 hippocampal neurons to evaluate the role of p70 S6K activity on Trim32 and MOV10
438 expression in the context of synaptic downscaling. Similar to rapamycin treatment, the
439 inhibition of p70 S6K phosphorylation prevented Trim32 translation and the subsequent
440 degradation of MOV10 upon bicuculline-induced hyperactivity (Figure 7J-L). These
441 observations showed that the activation of p70 S6K by mTORC1 is a key determinant
442 regulating the concerted translation of Trim32 and the degradation of MOV10 in downscaling.

443

444 **MOV10 degradation is sufficient to invoke downscaling of AMPARs**

445

446 MOV10 degradation in response to chronic bicuculline treatment made us enquire whether its
447 loss alone was sufficient to cause pervasive changes in the miRISC to effectuate synaptic
448 downscaling. We used lentivirus-mediated RNAi of MOV10 to mimic hyperactivity-driven
449 MOV10 degradation. Intensity of sGluA1/A2 puncta that co-localized with PSD95 was
450 analyzed following MOV10 knockdown (DIV21-24). We observed that loss of MOV10 reduced
451 the expression of sGluA1 (35.03 ± 9.35 % for shRNA#1, p<0.01 and 58.38 ± 10.27 % for
452 shRNA#2, p<0.01) and sGluA2 (49.4 ± 12.9% for shRNA#1, p<0.01) at the synapses (Figure
453 8A-D, S4), that recapitulated the re-distribution of sGluA1/sGluA2 in neurons under chronic

454 bicuculline treatment (Figure 2C-D). The knockdown of MOV10 reduced mEPSC amplitude
455 (3.43± 0.16 pA for shRNA#1 and 4.35± 0.14 pA for shRNA#2, $p<0.01$) but not frequency
456 (Figure 8E-G), an observation that mirrors synaptic downscaling (Figure 1E).
457 We examined whether MOV10 knockdown could further influence synaptic strength
458 effectuated by bicuculline. Bicuculline treatment did not further decrease the amplitude of
459 mEPSCs recorded from neurons expressing MOV10 shRNAs (Figure 8H – I). This observation
460 indicates that effect of MOV10 knockdown overrides the effect of bicuculline. We then
461 overexpressed myc-tagged MOV10 in hippocampal neurons and measured their synaptic
462 activity. Bicuculline treatment led to an enhancement of mEPSC amplitude (1.64 ± 0.14 pA
463 increase, $p<0.0001$) (Figure 8K – L) in neurons overexpressing MOV10 but not mEPSC
464 frequency (Figure 8K and 8M). Our data shows that the overexpression of MOV10 partially
465 occludes synaptic downscaling.

Figure: 8

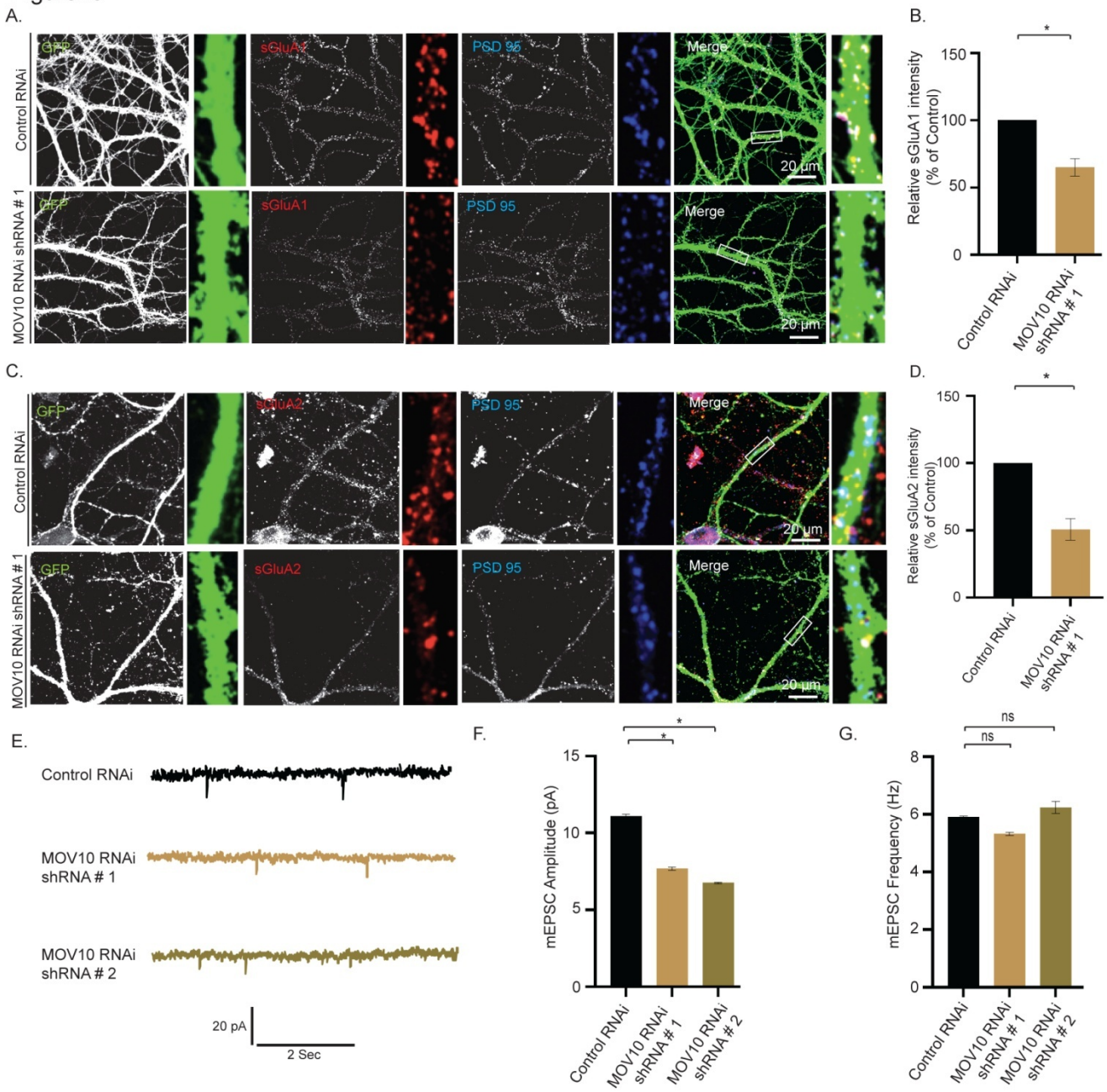
A.
Control RNAi
MOV10 RNAi shRNA # 1
GFP
sGluA1
PSD 95
Merge
20 µm
B.
Relative sGluA1 intensity (% of Control)
150
100
50
0
*
Control RNAi
MOV10 RNAi shRNA # 1
C.
sGluA2
D.
Relative sGluA2 intensity (% of Control)
E.
Control RNAi
MOV10 RNAi shRNA # 1
MOV10 RNAi shRNA # 2
20 pA
2 Sec
F.
mEPSC Amplitude (pA)
15
10
5
0
G.
mEPSC Frequency (Hz)
8
6
4
2
ns

466

Figure: 8

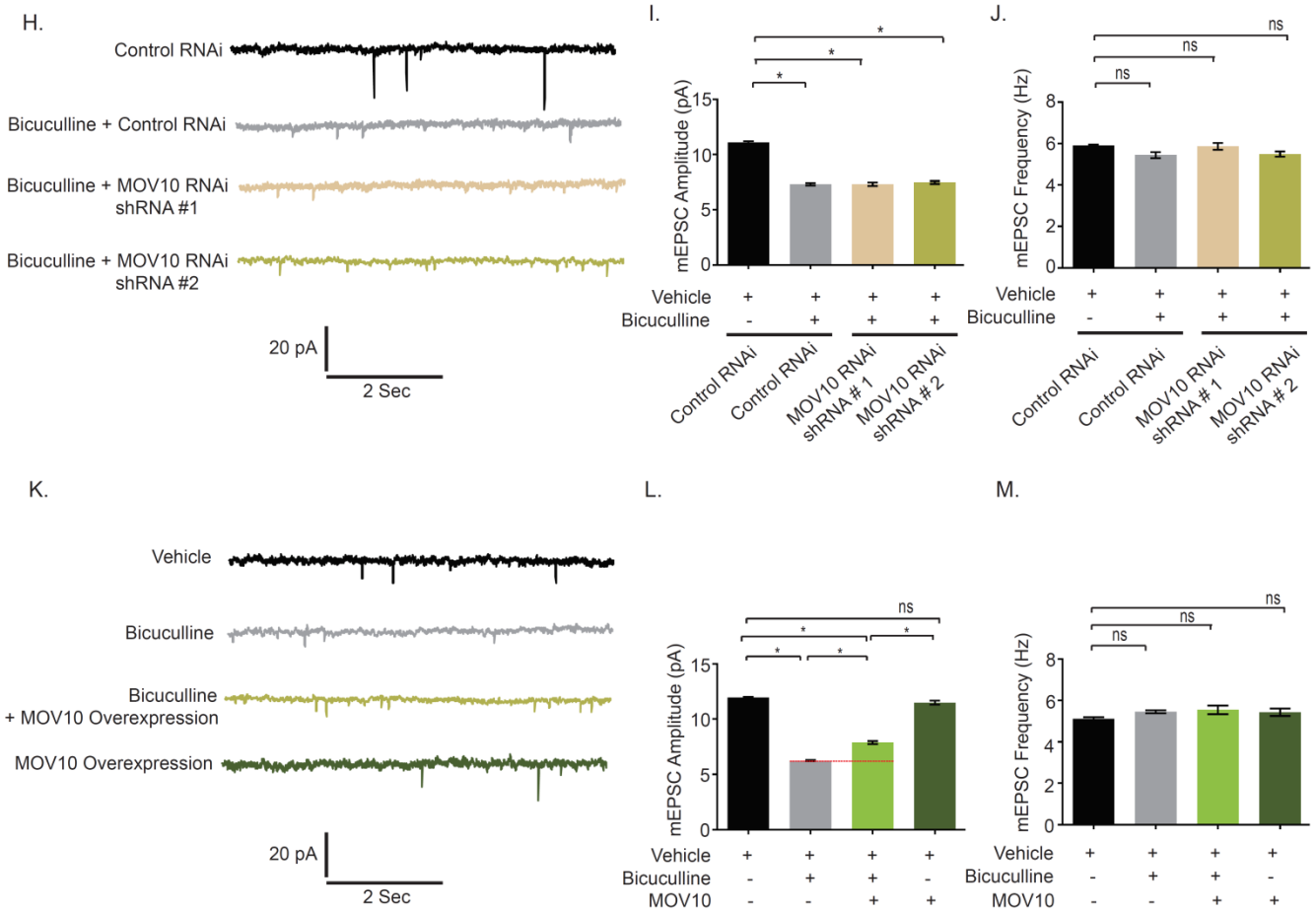

Figure 8: MOV10 modulates abundance of sAMPARs during synaptic downscaling

(A-D) High magnification images of neurons transduced with lentivirus co-expressing EGFP and shRNA against MOV10 or non-targeting shRNA showing expression of sGluA1 (A) or sGluA2 (C) (red), PSD95 (blue), GFP (green) and GFP/sGluA1/PSD95 or GFP/sGluA2/PSD95 (merged). Quantitation of normalized intensity of synaptic sGluA1 (B) or sGluA2 (D). n=26 - 30, GluA1; n=12 – 15, GluA2. Data shown as Mean ± SEM. *p<0.01. One Way ANOVA and Fisher's LSD. Dendrite marked in white box was digitally amplified. See also Figure S4.

(E-G) mEPSC traces from neurons transduced with shRNAs against MOV10 or control shRNA (E). Mean mEPSC amplitude (F) and frequency (G). n=12 – 13. *p<0.01. ns, not significant. Data shown as Mean ± SEM. One Way ANOVA and Fisher's LSD.

(H-J) mEPSC traces from bicuculline or vehicle treated neurons transduced with shRNAs against MOV10 or control shRNA (H). Mean mEPSC amplitude (I) and frequency (J). n=12 – 18. *p<0.0001. ns, not significant. Data shown as Mean ± SEM. One Way ANOVA and Fisher's LSD.

482 (K-M) mEPSC traces from bicuculline treated neurons overexpressing myc-tagged MOV10 (K). Mean mEPSC
483 amplitude (L) and frequency (M). n=13 – 15. *p<0.0001. ns, not significant. Data shown as Mean ± SEM. One
484 Way ANOVA and Fisher's LSD. Dotted line indicates the difference in mEPSC amplitude recorded from neurons
485 overexpressing MOV10 or control neurons following bicuculline treatment. See also Figure S6.

486

487 **Trim32 is required for AMPAR-mediated downscaling**

488

489 We have examined the role of Trim32 in bicuculline-induced downscaling by measuring
490 synaptic activity following the loss of Trim32. Trim32 knockdown in bicuculline-treated neurons
491 led to an increase in mEPSC amplitude (2.82 ± 0.23 pA increase, p<0.0001), but did not show
492 any change in frequency as compared to neurons incubated with bicuculline alone (Figure 9A-
493 C). A modest but significant increase in mEPSC amplitude (1.65± 0.25 pA increase, p<0.0001)
494 was also detected from neurons expressing Trim32 shRNA as compared to control shRNA
495 without any activity (Figure 9A-B). We presume that this could be due to an increase in basal
496 MOV10 expression following Trim32 knockdown (Figure 6D-E). Consistent with patch clamp
497 recording data from MOV10 overexpressing neurons, a partial occlusion of bicuculline-induced
498 downscaling by Trim32 knockdown establishes the requirement of Trim32-MOV10 axis in
499 synaptic scaling. We examined the involvement of sAMPARs in regulation of Trim32-mediated
500 downscaling. We observed that Trim32 knockdown in bicuculline-treated neurons enhanced
501 both sGluA1 (31.35 ± 6.65% increase, p<0.04) (Figure 9D – E, 9H) and sGluA2 (88.99 ±
502 5.52% increase, p<0.0005) (Figure 9F – G, 9I) as compared to neurons treated with bicuculline
503 alone.

Figure: 9

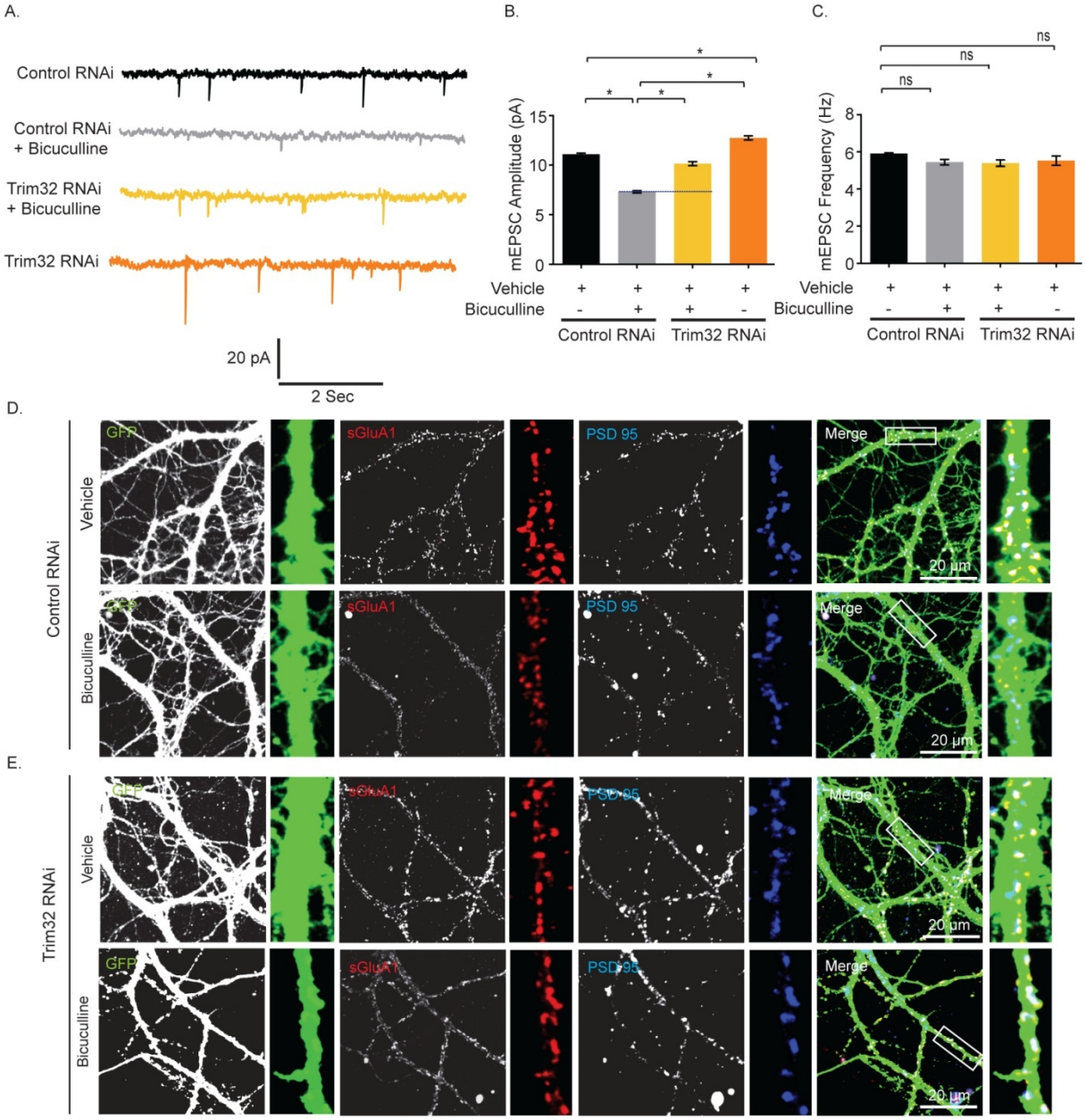
A.
Control RNAi
Control RNAi
+ Bicuculline
Trim32 RNAi
+ Bicuculline
Trim32 RNAi
20 pA
2 Sec
B.
mEPSC Amplitude (pA)
Vehicle
Bicuculline
Control RNAi
Trim32 RNAi
C.
mEPSC Frequency (Hz)
ns
D.
Control RNAi
Vehicle
Bicuculline
GFP
sGluA1
PSD 95
Merge
20 µm
E.
Trim32 RNAi

504

Figure: 9

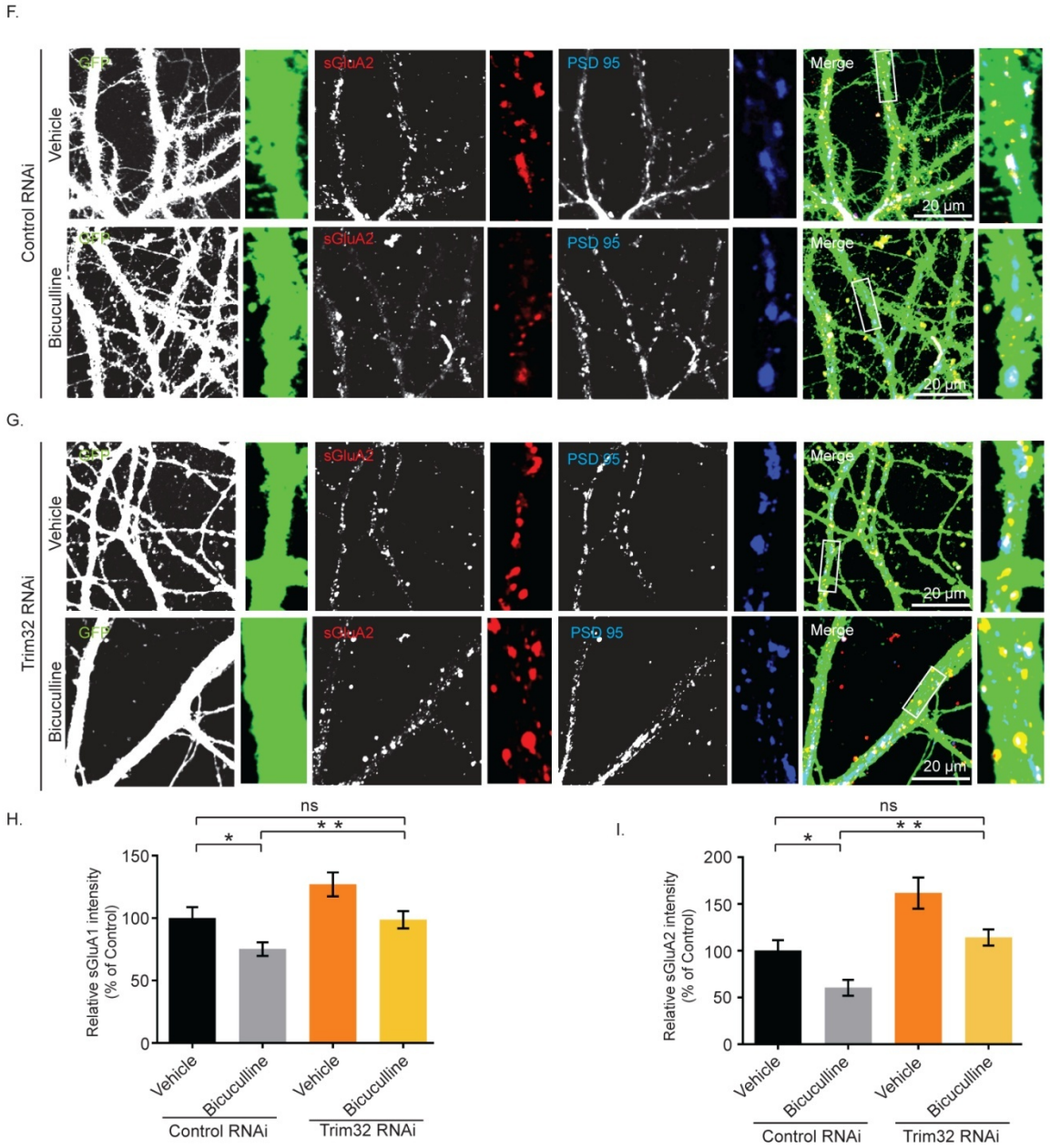

505

506 **Figure 9: Trim32 -mediated synaptic downscaling occurs *via* modulation of sAMPARs.**

507 (A-C) mEPSC traces from bicuculline or vehicle treated neurons transduced with shRNAs against Trim32 or
508 control shRNA (A). Mean mEPSC amplitude (B) and frequency (C). n=12 – 16. *p<0.0001. ns, not significant.
509 Data shown as Mean ± SEM. One Way ANOVA and Fisher's LSD. Dotted line indicates the difference in mEPSC
510 amplitude recorded from bicuculline treated neurons transduced with Trim32 shRNA or control shRNA.

511

512 (D-I) High magnification images of bicuculline or vehicle treated neurons transduced with lentivirus co-expressing
513 EGFP and shRNA against Trim32 or non-targetting shRNA showing expression of sGluA1 (D-E) or sGluA2 (F-G)
514 (red), PSD95 (blue), GFP (green) and GFP/sGluA1/PSD95 or GFP/sGluA2/PSD95 (merged). Quantitation of
515 normalized intensity of synaptic sGluA1 (H) or sGluA2 (I). n=30 - 40 for GluA1; n=23 – 36 for GluA2. Data shown
516 as Mean ± SEM. *p<0.02, **p<0.0001 for sGluA1. *p<0.006, **p<0.0005 for sGluA2. One Way ANOVA and
517 Fisher's LSD. Dendrite marked in white box was digitally amplified. See also Figure S5.
518
519

520 Similar to increase in mEPSC amplitude following Trim32 knockdown, our data showed an
521 increase in sGluA1 (27.009 ± 7.72%, p<0.04) and sGluA2 (61.63 ± 10.47%, p<0.007) in
522 Trim32 RNAi neurons. (Figure 9H – I). Comprehensively, our data demonstrates a regulatory
523 control of synaptic downscaling by the Trim32-MOV10 axis that modulates sAMPAR
524 expression.

525

526 **Trim32-MOV10 axis regulates Arc expression during synaptic downscaling**

527

528 How MOV10 degradation leads to the removal of sAMPARs to regulate synaptic downscaling?
529 Arc/Arg3.1, an immediate early gene, has been shown to be dynamically regulated by chronic
530 changes in synaptic activity, and evokes synaptic scaling [38]. Overexpression of Arc
531 decreases sAMPARs *via* endocytosis whereas its knockdown increases them [39]. Arc
532 expression has been shown to be regulated by diverse mechanisms including translational
533 control that involves miRNAs [40,41,42]. Since we found a decrease of sAMPAR distribution
534 on MOV10 knockdown, we investigated the correlation between MOV10 and Arc expression.
535 We observed that the loss of MOV10 enhanced Arc (113.1 ± 15.7% increase, p<0.002 for
536 shRNA # 1 and 173.8 ± 7.45% increase, p<0.0001 for shRNA # 2) (Figure 10A-B). The extent
537 of increase in Arc protein was commensurate with the degree of MOV10 knockdown (Figure

538 10A). We also observed that this differential enhancement of Arc protein was reflected in the
539 proportionate removal of sAMPARs and the concomitant decrease in mEPSC amplitude
540 (Figure 8F). Bicuculline-induced chronic hyperactivity, which degrades MOV10, also enhanced
541 Arc expression (132.1 ± 27.45% increase, $p<0.04$) (Figure 10C-D). This activity-driven
542 increase was blocked by the inhibition of mTORC1 with rapamycin (100nM, 24 hours) whereas
543 rapamycin treatment alone had no effect (Figure 10C-D).
544 Arc expression has been shown to be regulated by both transcriptional and post-transcriptional
545 control [42]. Post-transcriptional control of Arc expression is regulated by its 3'UTR that
546 contains multiple miRNA binding sites [40]. We explored the mechanism of mTORC1-
547 dependent Arc expression involving Trim32-MOV10 axis. We used an Arc-3'UTR fused
548 luciferase reporter (Arc-Luc) to assess Arc expression from bicuculline-treated neurons
549 following Trim32 and MOV10 knockdown. We found that the bicuculline-induced enhancement
550 of reporter activity (61.1 ± 3.24% increase, $p<0.0003$) was prevented by Trim32 knockdown
551 (Figure 10E) whereas MOV10 knockdown alone was sufficient to increase reporter activity
552 under basal conditions (77.34 ± 7.78% increase, $p<0.002$). Loss of MOV10 in bicuculline-
553 treated neurons did not enhance Arc-Luc reporter activity further as compared to bicuculline-
554 treated neurons (Figure 10E). This observation is consistent with our electrophysiology data
555 demonstrating that MOV10 knockdown in bicuculline-treated neurons did not elicit further
556 reduction in mEPSC amplitude when compared to neurons treated with bicuculline alone
557 (Figure 8I).

Figure 10

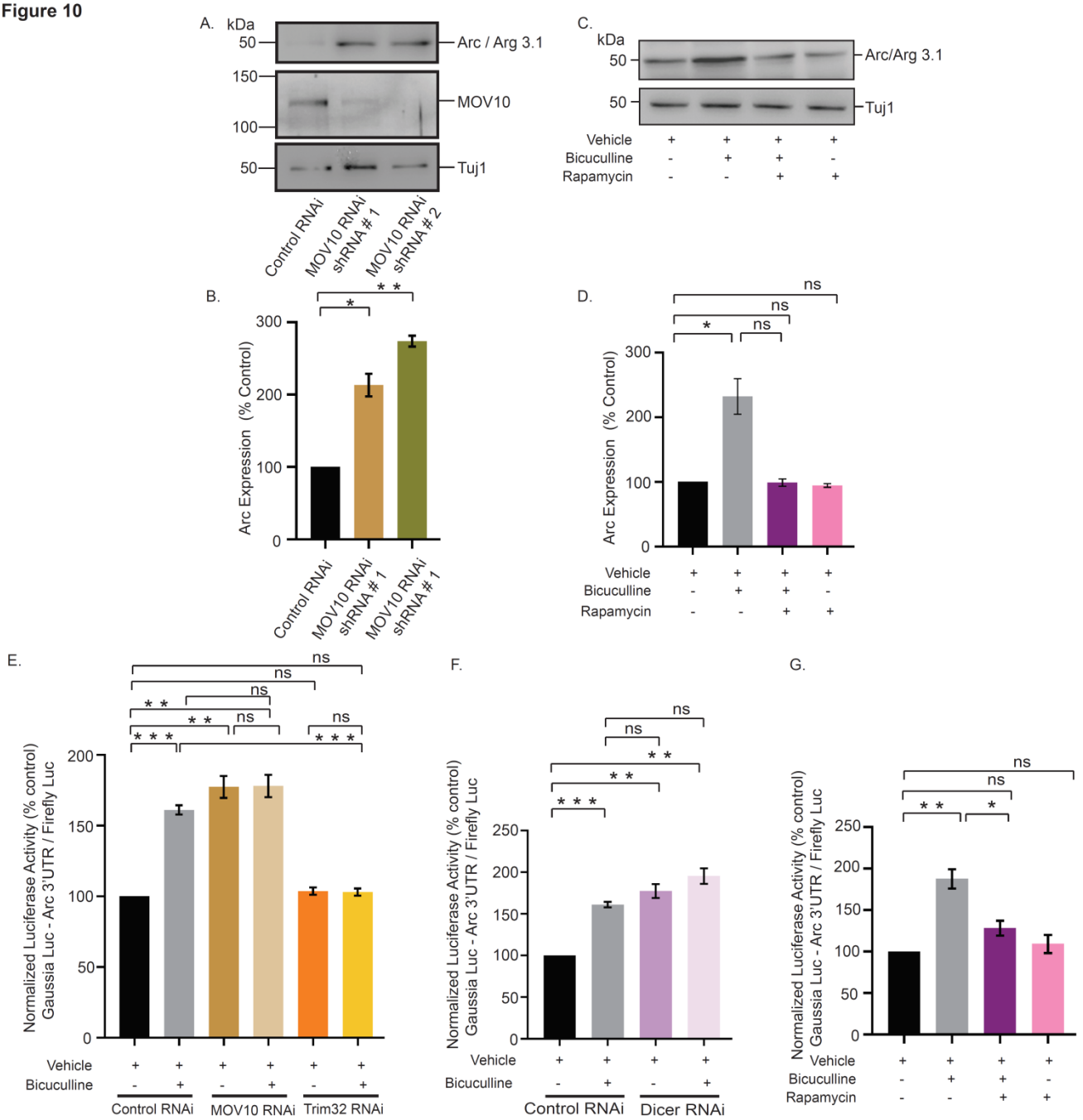

558

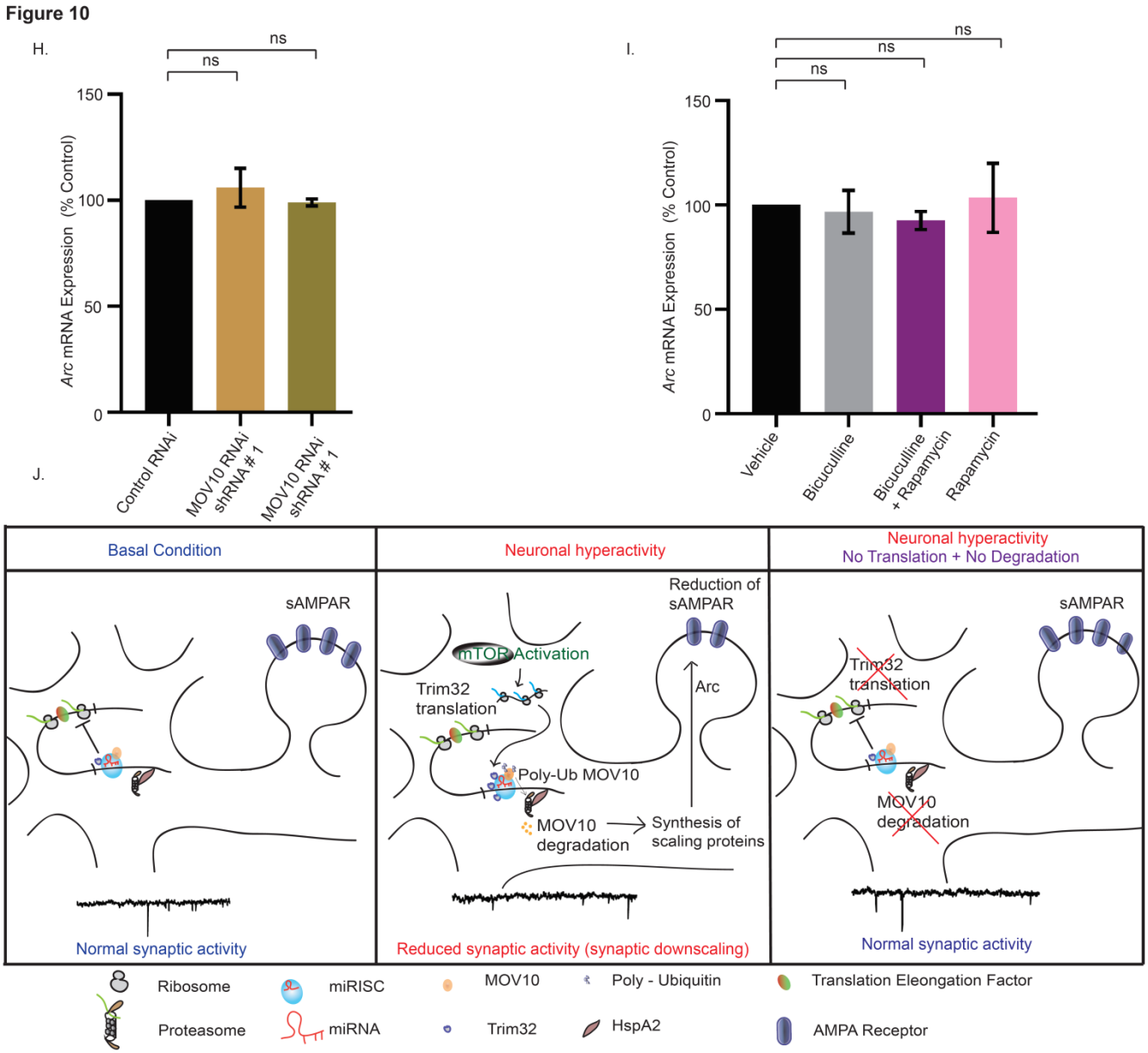

Figure 10: mTORC1-mediated regulation of Arc expression upon chronic hyperactivity involves MOV10.

(A-B) Western blot analysis showing the Arc protein level after MOV10 knockdown in neurons infected with lentivirus expressing two different shRNAs against MOV10 (A). Quantitation of Arc expression (B). n=6.* $p<0.002$, **$p<0.0001$. Data shown as Mean ± SEM. One Way ANOVA and Fisher's LSD.

(C-D) Western blot analysis of neurons treated with bicuculline in presence or absence of rapamycin showing the expression of Arc protein (C). Quantitation of Arc expression (D). n=3. *$p<0.04$. Data shown as Mean ± SEM. One Way ANOVA and Fisher's LSD.

568 (E-F) Quantitation of luciferase reporter expression from vehicle or bicuculline-treated neurons transduced with
569 lentivirus expressing shRNA against MOV10 and Trim32 (E), Dicer (F). n=4. **p<0.002, ***p<0.0003, ns, not
570 significant. Data shown as Mean ± SEM. One Way ANOVA and Fisher's LSD. See also Figure S6.
571
572 (G) Quantitation of luciferase reporter expression from vehicle or bicuculline-treated neurons in presence or
573 absence of rapamycin. n=7. **p<0.00, *p<0.04, ns, not significant. Data shown as Mean ± SEM. One Way
574 ANOVA and Fisher's LSD.
575
576 (H-I) Quantitation of qPCR analysis of Arc mRNA expression in neurons expressing shRNA against MOV10 or
577 control shRNA. n=3. ns, not significant. Data shown as Mean ± SEM. One Way ANOVA (H). Quantitation of qPCR
578 analysis of Arc mRNA expression in bicuculline-treated neurons in presence or absence of rapamycin (I). n=4. ns,
579 not significant. Data shown as Mean ± SEM. One Way ANOVA (I).
580
581 (J) Schematic representation showing maintenance of homeostatic synaptic activity by coordinated control of
582 protein synthesis and degradation that modulates composition of miRISC.

583
584 Since Dicer is a key component of the miRISC, its knockdown would definitely result in
585 pervasive miRISC remodeling and allow us to confirm whether miRISC remodeling has a role
586 in regulating Arc expression. Hence, we tested Arc-Luc reporter activity following Dicer
587 knockdown and found that similar to loss of MOV10, Dicer knockdown alone was sufficient to
588 enhance Arc-Luc reporter activity under basal conditions (77.4 ±8.31% increase, p<0.002)
589 (Figure 10F) and this enhancement was comparable to bicuculline-induced reporter activity
590 (77.4 ± 8.31 % increase in Dicer knockdown neurons *vs.* 61.1 ± 3.24% increase in bicuculline-
591 treated neurons) (Figure 10F). Similar to our western blot data (Figure 10C-D), we observed
592 that the bicuculline-induced enhancement of Arc-Luc activity (87.6 ± 11.64% increase,
593 p<0.002) was prevented by the application of rapamycin. Application of rapamycin alone did
594 not show any change. (Figure 10G).
595 To explore whether Arc was regulated by transcription during synaptic downscaling, we
596 checked Arc mRNA expression in bicuculline treated neurons after MOV10 knockdown and

597 after mTORC1 inhibition. qRT-PCR analysis showed no detectable change in Arc transcript
598 levels upon MOV10 knockdown or bicuculline-induced hyperactivity in presence or absence of
599 rapamycin (Figure 10I). Taken together, our data demonstrates that the bicuculline-induced
600 downscaling of synaptic strength occurs *via* an mTORC1-mediated Trim32 translation-
601 dependent MOV10 degradation involving removal of sAMPARs *via* Arc (Figure 10J).
602

603 ## Discussion

604

605 Here we provide empirical evidence emphasizing that synchrony between protein synthesis
606 and proteasomal activity is critical to establish homeostasis at synapses. We used a paradigm
607 of chronic network hyperactivity to invoke downscaling and determined that a) translation and
608 degradation apparatuses directly interact with each other and are tethered together by RNA
609 scaffolds; b) it is the translation of Trim32 that drives the degradation of MOV10 to cause
610 miRISC remodeling, thus the current paradigm is an example of translation preceding
611 degradation; c) miRISC is a key node in the translation-degradation axis, with the mTORC1-
612 p70 S6K pathway being the upstream signaling component and a part of the 'sensor'
613 machinery, and Arc-induced removal of sAMPARs being the final effectors of downscaling.
614

615 **Co-regulation of protein synthesis and degradation drives AMPAR-mediated synaptic**
616 **downscaling**

617 We find that chronic perturbation of either translation or proteasomal activity occludes synaptic
618 homeostasis, whereas homeostasis remains unperturbed when there is simultaneous inhibition
619 of both (Figure 1). Chronic application of bicuculline along with either lactacystin or anisomycin
620 leads to alterations of mEPSC amplitude that exactly mirror observations where bicuculline is

621 absent (Figure 1B *vs* Figure 1E). Thus, the effects of bicuculline-induced changes to the
622 existing proteome are overshadowed by those accomplished by the individual action of the
623 proteasome or the translation machinery (Figures 1). The importance of these observations is
624 multi-faceted; it establishes that, i) congruent protein synthesis and degradation pathways
625 regulate synaptic scaling; ii) the constancy of the proteomic pool in the presence of lactacystin
626 and anisomycin renders the effect of any network destabilizing stimuli like bicuculline to be
627 redundant, and iii) bicuculline induced changes in the proteome predominantly affects the
628 physiology of the post-synaptic compartment.
629 Our observations echo previous findings in Hebbian plasticity; wherein, protein synthesis
630 during LTP/LTD was required to counter the changes in the proteomic pool triggered by protein
631 degradation. The blockade of L-LTP accomplished by inhibiting protein synthesis was revoked
632 on the simultaneous application of proteasomal blockers and translational inhibitors [43].
633 Abrogation of proteasomal activity allowed mGluR-dependent LTD to proceed when protein
634 synthesis was co-inhibited [44]. These observations emphasize the existence of a proteostasis
635 network that enable compositional changes to the proteome in contexts of acute or chronic
636 changes in synaptic function [32,45,46]. As LTP and LTD modify the cellular proteome through
637 the simultaneous recruitment of protein synthesis and degradation; it stands to reason that
638 homeostatic scaling mechanisms may also employ a functional synergy of the two to
639 recompense for the changes brought about by unconstrained Hebbian processes.
640 AMPAR-mediated currents decrease more than NMDAR currents during chronic network
641 hyperactivity [14,18] and unlike NMDARs, the turnover of AMPARs is translation-dependent
642 [47]. The reduced level of sAMPARs following chronic hyperactivity is reset to basal level by
643 the co-application of protein synthesis and proteasome inhibitors, suggesting that the

644 combined action of translation and degradation affects post-synaptic scaling specifically
645 through sAMPARs. Similar to the observations in synaptic upscaling [13], restricting changes
646 to the sAMPAR abundance by the inhibition of GluA2-endocytosis using $GluA2_{3Y}$ peptide also
647 blocks synaptic downscaling (Figure 2); reinforcing that AMPARs indeed remain the end-point
648 effectors despite changes to the proteome.
649
650 **Association of the translation and degradation apparatus is RNA-dependent**
651
652 The co-localization of polyribosomes and proteasomes in neuronal sub-compartments
653 suggests that for translation and proteasomal degradation to work in tandem, physical
654 proximity between the two modules cannot be ruled out [30,31]. Polysome analysis showed
655 the co-sedimentation of members of the 19S proteasome (Rpt1, Rpt3 and Rpt6 subunits) and
656 the 20S proteasome (α7 subunit) along with translation initiation factors such as eIF4E and
657 p70S6 kinase, a downstream effector of mTORC1. Abrogation of the sedimentation pattern in
658 the presence of RNase or EDTA, is indicative of an RNA-dependent direct interaction between
659 translation and protein degradation (Figure 3). RNAse treatment also abolished the direct
660 interaction between proteasome subunits and translation regulators within the polysome,
661 suggesting that actively-translating transcripts act as a scaffold to link the translation and
662 proteasome machineries (Figure 4). Such existence of direct interaction between
663 polyribosomes and catalytically active proteasomes allows close temporal coordination
664 between translation and protein degradation.
665

666 Does chronic hyperactivity influence the association of proteasome and translation regulators
667 within the polysome? The bicuculline-induced enrichment of 26S proteasome, phosphorylated
668 S6, p70 S6 kinase and its phosphorylated form, and eEF2 in polysomes is indicative of activity-
669 dependent proximity between the translation and degradation machineries (Figure 5).
670 Interestingly, eEF2 has been previously characterized as a biochemical sensor for synaptic
671 scaling [17]. Trim32, an E3 ligase, was enriched in polysomes whereas MOV10 and Argonaute
672 to be depleted from polysomes on chronic bicuculline treatment. Trim32 and MOV10 were also
673 present in polysomes in basal conditions (Figure 5).
674 Previously, MOV10 and Trim32 have been implicated in miRISC-independent functions to
675 modulate RNA modification [48], stability [49] and transcription [50] respectively. Density
676 gradient fractionations of cytoplasmic lysates obtained from non-neuronal systems have
677 revealed that Argonaute cosedimented with miRNAs in polysome fractions [51,52]. MOV10
678 was also found associated with polysomes [24]. Interestingly, Trim32 and Argonaute co-
679 immunoprecipitated with MOV10 from neurons suggesting that they closely interact with each
680 other and are members of the miRISC (Figure 4F). Apart from this observation, polysome
681 association of Trim32, MOV10 and Argonaute is bicuculline responsive (Figure 5). We found
682 that chronic bicuculline stimulation triggers a change in the association of Trim32 and MOV10
683 with Argonaute (Figure 6). Evidence of their direct physical interaction led us to infer that both
684 MOV10 and Trim32 are part of the miRISC. Hence, association of Argonaute, Trim32 and
685 MOV10 with polysome can be representative of the association of the miRISC with polysomes;
686 at-least in the context of synaptic downscaling.
687

688 How does the proteasome remain associated with actively translating mRNAs? We have
689 identified that HspA2 (Hsp70 family), a chaperone protein, remains tethered to proteasomes
690 and polysomes (Figure 4-5). Hsp70 family of proteins is known to influence both the synthesis
691 and degradation of proteins by their association with 26S proteasomal subunits [53],
692 translation initiation factors [54]. Hspa2 has been shown to be an interacting partner of the
693 miRISC [55]. Therefore, HspA2 could potentially function as a proteostasis coordinator which
694 includes members of the proteasome, translation regulators and chaperon proteins.
695
696 **Bicuculline mediated regulation of Trim32 and MOV10 causes miRISC remodeling**
697 **during downscaling.**
698
699 We found that during chronic bicuculline treatment, translation of Trim32 precedes the
700 degradation of MOV10. The alternative possibility that MOV10 degradation leads to increased
701 *de novo* translation of Trim32, is not supported, since protein synthesis inhibition by
702 anisomycin leads to MOV10 rescue (Figure 6). Loss of Trim32 prevented bicuculline-induced
703 polyubiquitination and subsequent degradation of MOV10, suggesting that Trim32 is the only
704 E3 ligase marking MOV10 for degradation during synaptic scaling (Figure 6).
705 Immunoprecipitation of Argonaute from cultured neurons following chronic bicuculline
706 treatment showed MOV10 to be depleted and Trim32 to be enriched, without any change in
707 Dicer expression. Previously, changes to the components of the miRISC have been termed as
708 miRISC remodeling [25] and such compositional changes result in alteration of miRISC activity
709 [23,56]. Our observations therefore emphasize that such compositional changes within the
710 miRISC, or miRISC remodeling, is effectuated through the reciprocal translational-degradation

711 of the Trim32-MOV10 axis. Prolonged bicuculline treatment also did not influence the
712 Argonaute level, indicating that specific components of the silencing complex are targeted
713 during scaling (Figure 6 and S3).
714 A recent study has demonstrated that a slow turnover of plasticity proteins (measured at 1,3
715 and 7 days in cultured neurons) is essential to create long-term changes to the neuronal
716 proteome during both up and down-scaling [57]. The authors have argued that the slow
717 turnover rate is more energy-saving and therefore a preferred cellular mechanism. At the same
718 time, this study also identifies a very small fraction of previously reported scaling factors with
719 fast turnover rates specifically influencing up- and down- scaling. Our reports support the latter
720 findings, where we observe that both the increase in Trim32 synthesis and the resultant
721 degradation of MOV10 happen within 24 hours during synaptic downscaling, suggesting a fast
722 turnover. As both MOV10 and Trim32 are part of the miRISC, their fast turnover rates seems
723 plausible, considering that participation of the miRISC is mandatory to relieve the translational
724 repression of several transcripts encoding plasticity proteins and needs to happen rapidly in
725 order to boost changes to the proteome. Although in terms of energy expenditure the
726 coordinated regulation of translation and degradation is expensive, this cellular trade-off may
727 be necessary to trigger the remodeling of a very limited number of master regulators of the
728 neuronal proteome, such as miRISC, during synaptic downscaling.
729
730 **mTORC1 dependent Trim32 translation-driven MOV10 degradation is sufficient to cause**
731 **synaptic downscaling.**
732

733 What post-synaptic signaling cascade triggers Trim32 translation? We find that chronic
734 bicuculline induction triggers the mTORC1-dependent synthesis of Trim32 with the consequent
735 degradation of MOV10 that is a prerequisite for bicuculline-induced downscaling (Figure 7).
736 Although both p70 S6 kinase and 4EBP2 are downstream effectors of mTORC1, we find that
737 the phosphorylation of p70 S6 kinase exclusively drives Trim32 translation.
738
739 After investigating the upstream regulators of the Trim32-MOV10 axis, we focused on
740 identifying the downstream factors that lead to loss of surface AMPAR abundance during
741 downscaling. Most studies have determined the influence of single miRNAs in regulating
742 AMPAR distribution during scaling; however, they have been inadequate in providing a holistic
743 view of the miRNA-mediated control of sAMPAR abundance [19–22]. MiRNA function has
744 been shown to be directly co-related with miRISC activity [23,56]. Hence, we explored how
745 miRISC remodeling contributes to synaptic downscaling *via* the regulation of AMPARs. We
746 found that loss of MOV10 function single-handedly accounted for the loss of sGluA1/A2,
747 accompanied by commensurate decrease in mEPSC amplitude under basal conditions,
748 effectively recapitulating the post-synaptic events during downscaling (Figure 8). MOV10
749 knockdown did not reduce mEPSC amplitude further following bicuculline treatment. This
750 observation indicates that the loss of MOV10 sets the threshold point of synaptic strength and
751 chronic hyperactivity cannot override this set point (Figure 8).
752 We genetically manipulated MOV10 and Trim32 so that their expression becomes opposite to
753 that observed during scaling, i.e, we overexpressed MOV10 and performed Trim32 RNAi. We
754 found, that MOV10 overexpression led to a partial occlusion of downscaling (Figure 8). Though
755 myc-tagged MOV10 was amenable for degradation by UPS, yet sustained increased levels of

756 the ectopically expressed MOV10 even after bicuculline treatment was sufficient to cause
757 partial impairment of downscaling. Chronic bicuculline treatment post Trim32 RNAi resulted in
758 an increase in mEPSC amplitudes in neurons, which is commensurate with the enhancement
759 of sAMPARs (Figure 9). Thus, Trim32 knockdown caused a partial impairment of downscaling.
760 We also observed that Trim32 RNAi under basal conditions causes a modest but statistically
761 significant increase in mEPSC amplitude (Figure 9). We anticipate that this could be due to
762 enhanced MOV10 expression following Trim32 knockdown under basal condition (Figure 6E).
763 Since the reversal of Trim32 and MOV10 expression levels lead to the partial abolishment of
764 downscaling in neurons upon chronic bicuculline treatment, we infer that the Trim32-MOV10
765 mediated miRISC remodeling is pivotally positioned to regulate synaptic scaling.
766

767 **mTORC1 triggers miRISC remodeling to regulate Arc synthesis during downscaling**

768 Similar to previous observation [38], our study shows that bicuculline-induced hyperactivity
769 enhances Arc protein, a known regulator of AMPAR removal from synapses. Enhanced Arc
770 translation during chronic bicuculline treatment was blocked by rapamycin, suggesting a
771 regulatory role of mTORC1 in its expression. Furthermore, increase in Arc translation (Figure
772 10) and concomitant reduction of sAMPARs after loss of MOV10 (Figure 8) demonstrates Arc
773 to be a crucial intermediate between MOV10 degradation and synaptic downscaling.
774 How Arc expression is regulated during chronic hyperactivity? Our data demonstrates that in
775 the context of downscaling, rapamycin-sensitive Arc expression is driven by post-
776 transcriptional control rather than transcriptional regulation. Chronic hyperactivity-dependent
777 enhanced expression of Arc requires the 3'UTR of the transcript containing multiple miRNA
778 binding sites [40], suggesting an involvement of miRISC in scaling. Trim32 knockdown or

779 mTORC1 inhibition prevents the bicuculline-induced increase in Arc reporter expression. We
780 observed that loss of Trim32 alone does not affect the reporter activity, but MOV10 knockdown
781 is sufficient to enhance it (Figure 10). Since MOV10 RNAi mimics the bicuculline-induced
782 reduction of MOV10 during synaptic hyperactivity, and MOV10 regulates miRISC function, we
783 believe that miRISC remodeling is a key determinant of Arc expression. To further enquire
784 whether change of miRISC activity is sufficient to cause increased Arc expression, we
785 performed the RNAi of Dicer, another key component of the miRISC. Similar to MOV10, loss of
786 Dicer has been shown to inhibit miRISC function [56]. Enhanced Arc reporter activity upon
787 Dicer knockdown emphasizes the requirement of miRISC function in regulating Arc (Figure
788 10).Arc mRNA levels remain unaffected upon chronic hyperactivity in presence or absence of
789 rapamycin as well as knockdown of MOV10 (Figure 10), suggesting that transcription does not
790 play a role in regulating Arc in the context of bicuculline-induced downscaling.
791
792 In contrast to chronic hyperactivity driven loss of MOV10, its polyubiquitination and subsequent
793 localized degradation at active synapses has been shown to occur within minutes upon
794 glutamate stimulation of hippocampal neurons in culture or during fear memory formation in
795 amygdala [23,58]. These observations indicate that MOV10 degradation is a common player
796 involved in both Hebbian and homeostatic forms of plasticity. Hebbian plasticity paradigms
797 triggers homeostatic scaling in neurons as a compensatory mechanism [5]; these two
798 opposing forms of plasticity therefore must involve a combination of overlapping and distinct
799 molecular players. Our data demonstrates the requirement of a rapamycin-sensitive, MOV10
800 degradation-dependent Arc translation in homeostatic scaling that is distinct from the
801 rapamycin-insensitive dendritic translation of Arc occurring during Hebbian plasticity [59]. We

802 speculate that homeostatic and Hebbian plasticity engages distinct signaling pathways that
803 converge at miRISC remodeling.
804
805 Though most homeostatic scaling studies including ours used hippocampal neurons in culture
806 to investigate the mechanistic details, the use of this model leaves a lacuna to evaluate how
807 input-specific gene expression control at selective synapses during Hebbian plasticity
808 influences compensatory changes across all synaptic inputs to achieve network homeostasis.
809 Therefore, physiological relevance of homeostatic scaling needs to be studied in association
810 with Hebbian plasticity in order to delineate factors contributing to proteostasis involving cell
811 intrinsic and extrinsic variables within a circuit.
812
813 **Author Contributions**
814 S.B and S.S designed the study. S.S., and B.S. performed all experiments. S.S., B.S., and
815 S.B. analyzed the data. J.P.C. provided critical comments on electrophysiology experiments
816 and manuscript. S.V.S.M gave comments on manuscript. S.S. and S.B wrote the manuscript.
817
818 **Acknowledgement:**
819 We thank Dr. Dipanjan Roy for helpful discussions, Addgene for lentiviral vectors; Ken Kosik
820 for MOV10 shRNA and myc-MOV10 constructs; Clive Bramham for Arc 3'UTR fused luciferase
821 reporter construct; microscope facility of Regional Centre for Biotechnology, India; Rohini Roy
822 for Trim32 RNAi construct; Utsav Mukherjee, Premkumar Palanisamy, Gourav Sharma,
823 Anupam Das and Surajit Chakraborty for technical assistance and animal maintenance;
824 Karthick Ravichandran for helping with polysome fractionation. . This work is supported by

825 Ramalingaswami Fellowship (BT/RLF/Re-entry/32/2011) from the Department of
826 Biotechnology, Government of India and National Brain Research Centre core fund to S.B.
827
828 Authors declare no conflict of interest

References:

1. Burrone J, Murthy VN. Synaptic gain control and homeostasis. Current Opinion in Neurobiology. 2003. pp. 560–567. doi:10.1016/j.conb.2003.09.007

2. Keck T, Toyoizumi T, Chen L, Doiron B, Feldman DE, Fox K, et al. Integrating Hebbian and homeostatic plasticity: The current state of the field and future research directions. Philosophical Transactions of the Royal Society B: Biological Sciences. 2017. doi:10.1098/rstb.2016.0158

3. Turrigiano GG. The dialectic of hebb and homeostasis. Philos Trans R Soc B Biol Sci. 2017;372. doi:10.1098/rstb.2016.0258

4. Turrigiano GG, Nelson SB. Homeostatic plasticity in the developing nervous system. Nature Reviews Neuroscience. 2004. pp. 97–107. doi:10.1038/nrn1327

5. Vitureira N, Goda Y. The interplay between hebbian and homeostatic synaptic plasticity. Journal of Cell Biology. 2013. pp. 175–186. doi:10.1083/jcb.201306030

6. Pozo K, Goda Y. Unraveling mechanisms of homeostatic synaptic plasticity. Neuron. 2010. pp. 337–351. doi:10.1016/j.neuron.2010.04.028

7. Davis GW. Homeostatic control of neural activity: From phenomenology to molecular design. Annu Rev Neurosci. 2006;29: 307–323. doi:10.1146/annurev.neuro.28.061604.135751

8. Ibata K, Sun Q, Turrigiano GG. Rapid Synaptic Scaling Induced by Changes in Postsynaptic Firing. Neuron. 2008;57: 819–826. doi:10.1016/j.neuron.2008.02.031

9. Wierenga CJ, Walsh MF, Turrigiano GG. Temporal regulation of the expression locus of homeostatic plasticity. J Neurophysiol. 2006;96: 2127–2133. doi:10.1152/jn.00107.2006

10. Sutton MA, Taylor AM, Ito HT, Pham A, Schuman EM. Postsynaptic Decoding of Neural Activity: eEF2 as a Biochemical Sensor Coupling Miniature Synaptic Transmission to Local Protein Synthesis. Neuron. 2007;55: 648–661. doi:10.1016/j.neuron.2007.07.030

11. Henry FE, McCartney AJ, Neely R, Perez AS, Carruthers CJL, Stuenkel EL, et al. Retrograde changes in presynaptic function driven by dendritic mTORC1. J Neurosci. 2012;32: 17128–17142. doi:10.1523/JNEUROSCI.2149-12.2012

12. Henry FE, Wang X, Serrano D, Perez AS, Carruthers CJL, Stuenkel EL, et al. A unique homeostatic signaling pathway links synaptic inactivity to postsynaptic mTORC1. J Neurosci. 2018;38: 2207–2225. doi:10.1523/JNEUROSCI.1843-17.2017

13. Gainey MA, Hurvitz-Wolff JR, Lambo ME, Turrigiano GG. Synaptic scaling requires the GluR2 subunit of the AMPA receptor. J Neurosci. 2009;29: 6479–6489. doi:10.1523/JNEUROSCI.3753-08.2009

14. O'Brien RJ, Kamboj S, Ehlers MD, Rosen KR, Fischbach GD, Huganir RL. Activity-dependent modulation of synaptic AMPA receptor accumulation. Neuron. 1998;21: 1067–1078. doi:10.1016/S0896-6273(00)80624-8

15. Tatavarty V, Sun Q, Turrigiano GG. How to scale down postsynaptic strength. J Neurosci. 2013;33: 13179–13189. doi:10.1523/JNEUROSCI.1676-13.2013

16. Thiagarajan TC, Lindskog M, Tsien RW. Adaptation to synaptic inactivity in hippocampal neurons. Neuron. 2005;47: 725–737. doi:10.1016/j.neuron.2005.06.037

17. Sutton MA, Ito HT, Cressy P, Kempf C, Woo JC, Schuman EM. Miniature Neurotransmission Stabilizes Synaptic Function via Tonic Suppression of Local Dendritic Protein Synthesis. Cell. 2006;125: 785–799. doi:10.1016/j.cell.2006.03.040

18. Lissin D V., Gomperts SN, Carroll RC, Christine CW, Kalman D, Kitamura M, et al. Activity differentially regulates the surface expression of synaptic AMPA and NMDA glutamate receptors. Proc Natl Acad Sci U S A. 1998;95: 7097–7102. doi:10.1073/pnas.95.12.7097

19. Hou Q, Ruan H, Gilbert J, Wang G, Ma Q, Yao WD, et al. MicroRNA miR124 is required for the expression of homeostatic synaptic plasticity. Nat Commun. 2015;6. doi:10.1038/ncomms10045

20. Letellier M, Elramah S, Mondin M, Soula A, Penn A, Choquet D, et al. MiR-92a regulates expression of synaptic GluA1-containing AMPA receptors during homeostatic scaling. Nat Neurosci. 2014;17: 1040–1042. doi:10.1038/nn.3762

21. Rajman M, Metge F, Fiore R, Khudayberdiev S, Aksoy□Aksel A, Bicker S, et al. A microRNA□129□5p/Rbfox crosstalk coordinates homeostatic downscaling of excitatory synapses. EMBO J. 2017;36: 1770–1787. doi:10.15252/embj.201695748

22. Silva MM, Rodrigues B, Fernandes J, Santos SD, Carreto L, Santos MAS, et al. MicroRNA-186-5p controls GluA2 surface expression and synaptic scaling in hippocampal neurons. Proc Natl Acad Sci U S A. 2019;116: 5727–5736. doi:10.1073/pnas.1900338116

23. Banerjee S, Neveu P, Kosik KS. A Coordinated Local Translational Control Point at the Synapse Involving Relief from Silencing and MOV10 Degradation. Neuron. 2009;64: 871–884. doi:10.1016/j.neuron.2009.11.023

24. Kenny PJ, Zhou H, Kim M, Skariah G, Khetani RS, Drnevich J, et al. MOV10 and FMRP regulate AGO2 association with microRNA recognition elements We have identified a new mechanism for FMRP-mediated translational regulation through its association with MOV10. Cell Rep. 2014.

25. Schratt G. MicroRNAs at the synapse. Nature Reviews Neuroscience. 2009. pp. 842–849. doi:10.1038/nrn2763

26. Ehlers MD. Activity level controls postsynaptic composition and signaling via the ubiquitin-proteasome system. Nat Neurosci. 2003;6: 231–242. doi:10.1038/nn1013

27. Jakawich SK, Neely RM, Djakovic SN, Patrick GN, Sutton MA. An essential postsynaptic role for the ubiquitin proteasome system in slow homeostatic synaptic plasticity in cultured hippocampal neurons. Neuroscience. 2010;171: 1016–1031. doi:10.1016/j.neuroscience.2010.09.061

28. Schanzenbächer CT, Sambandan S, Langer JD, Schuman EM. Nascent Proteome Remodeling following Homeostatic Scaling at Hippocampal Synapses. Neuron. 2016;92: 358–371. doi:10.1016/j.neuron.2016.09.058

29. Schanzenbächer CT, Langer JD, Schuman EM. Time- and polarity-dependent proteomic changes associated with homeostatic scaling at central synapses. Elife. 2018;7. doi:10.7554/eLife.33322

30. Bingol B, Schuman EM. Activity-dependent dynamics and sequestration of proteasomes in dendritic spines. Nature. 2006;441: 1144–1148. doi:10.1038/nature04769

31. Ostroff LE, Fiala JC, Allwardt B, Harris KM. Polyribosomes redistribute from dendritic shafts into spines with enlarged synapses during LTP in developing rat hippocampal slices. Neuron. 2002;35: 535–545. doi:10.1016/S0896-6273(02)00785-7

32. Hanus C, Schuman EM. Proteostasis in complex dendrites. Nature Reviews Neuroscience. 2013. pp. 638–648. doi:10.1038/nrn3546

33. Schwamborn JC, Berezikov E, Knoblich JA. The TRIM-NHL Protein TRIM32 Activates MicroRNAs and Prevents Self-Renewal in Mouse Neural Progenitors. Cell. 2009;136: 913–925. doi:10.1016/j.cell.2008.12.024

34. Ma XM, Blenis J. Molecular mechanisms of mTOR-mediated translational control. Nature Reviews Molecular Cell Biology. 2009. pp. 307–318. doi:10.1038/nrm2672

35. Sanz E, Yang L, Su T, Morris DR, McKnight GS, Amieux PS. Cell-type-specific isolation of ribosome-associated mRNA from complex tissues. Proc Natl Acad Sci U S A. 2009;106: 13939–13944. doi:10.1073/pnas.0907143106

36. Shigeoka T, Jung H, Jung J, Turner-Bridger B, Ohk J, Lin JQ, et al. Dynamic Axonal Translation in Developing and Mature Visual Circuits. Cell. 2016;166: 181–192. doi:10.1016/j.cell.2016.05.029

37. Hay N, Sonenberg N. Upstream and downstream of mTOR. Genes Dev. 2004;18: 1926–1945. doi:10.1101/gad.1212704

38. Shepherd JD, Rumbaugh G, Wu J, Chowdhury S, Plath N, Kuhl D, et al. Arc/Arg3.1 Mediates Homeostatic Synaptic Scaling of AMPA Receptors. Neuron. 2006;52: 475–484. doi:10.1016/j.neuron.2006.08.034

39. Chowdhury S, Shepherd JD, Okuno H, Lyford G, Petralia RS, Plath N, et al. Arc/Arg3.1 Interacts with the Endocytic Machinery to Regulate AMPA Receptor Trafficking. Neuron. 2006;52: 445–459. doi:10.1016/j.neuron.2006.08.033

40. Wibrand K, Pai B, Siripornmongcolchai T, Bittins M, Berentsen B, Ofte ML, et al. MicroRNA regulation of the synaptic plasticity-related gene Arc. PLoS One. 2012;7. doi:10.1371/journal.pone.0041688

41. Paolantoni C, Ricciardi S, de Paolis V, Okenwa C, Catalanotto C, Ciotti MT, et al. Arc 3' UTR splicing leads to dual and antagonistic effects in fine-tuning arc expression upon BDNF signaling. Front Mol Neurosci. 2018;11. doi:10.3389/fnmol.2018.00145

42. Bramham CR, Worley PF, Moore MJ, Guzowski JF. The immediate early gene Arc/Arg3.1: Regulation, mechanisms, and function. J Neurosci. 2008;28: 11760–11767. doi:10.1523/JNEUROSCI.3864-08.2008

43. Fonseca R, Vabulas RM, Hartl FU, Bonhoeffer T, Nägerl UV. A Balance of Protein Synthesis and Proteasome-Dependent Degradation Determines the Maintenance of LTP. Neuron. 2006;52: 239–245. doi:10.1016/j.neuron.2006.08.015

44. Klein ME, Castillo PE, Jordan BA. Coordination between translation and degradation regulates inducibility of mGluR-LTD. Cell Rep. 2015;10: 1459–1466. doi:10.1016/j.celrep.2015.02.020

45. Jayaraj GG, Hipp MS, Ulrich Hartl F. Functional modules of the proteostasis network. Cold Spring Harb Perspect Biol. 2020;12. doi:10.1101/cshperspect.a033951

46. Cajigas IJ, Will T, Schuman EM. Protein homeostasis and synaptic plasticity. EMBO Journal. 2010. pp. 2746–2752. doi:10.1038/emboj.2010.173

47. Goold CP, Nicoll RA. Single-Cell Optogenetic Excitation Drives Homeostatic Synaptic Depression. Neuron. 2010;68: 512–528. doi:10.1016/j.neuron.2010.09.020

48. Warkocki Z, Krawczyk PS, Adamska D, Bijata K, Garcia-Perez JL, Dziembowski A. Uridylation by TUT4/7 Restricts Retrotransposition of Human LINE-1s. Cell. 2018;174: 1537-1548.e29. doi:10.1016/j.cell.2018.07.022

49. Gregersen LH, Schueler M, Munschauer M, Mastrobuoni G, Chen W, Kempa S, et al. MOV10 Is a 5’ to 3’ RNA Helicase Contributing to UPF1 mRNA Target Degradation by Translocation along 3’ UTRs. Mol Cell. 2014;54: 573–585. doi:10.1016/j.molcel.2014.03.017

50. Hillje AJ, Povlou MAS, Beckmann E, Worlitzer MMA, Bahnassawy L, LewejohannL, et al. TRIM32-dependent transcription in adult neural progenitor cells regulates neuronal differentiation. Cell Death & Disease. 2013,4: 1-13. doi:10.1038/cddis.2013.487

51. Nottrott S, Simard MJ, Richter JD. Human let-7a miRNA blocks protein production on actively translating polyribosomes. Nat Struct Mol Biol. 2006;13: 1108–1114. doi:10.1038/nsmb1173

52. Krichevsky AM, King KS, Donahue CP, Khrapko K, Kosik KS. A microRNA array reveals extensive regulation of microRNAs during brain development. Rna. 2003;9: 1274–1281. doi:10.1261/rna.5980303

53. Tai HC, Besche H, Goldberg AL, Schuman EM. Characterization of the brain 26S proteasome and its interacting proteins. Front Mol Neurosci. 2010;3. doi:10.3389/fnmol.2010.00012

54. Shalgi R, Hurt JA, Krykbaeva I, Taipale M, Lindquist S, Burge CB. Widespread Regulation of Translation by Elongation Pausing in Heat Shock. Mol Cell. 2013;49: 439–452. doi:10.1016/j.molcel.2012.11.028

55. Landthaler M, Gaidatzis D, Rothballer A, Chen PY, Soll SJ, Dinic L, et al. Molecular characterization of human Argonaute-containing ribonucleoprotein complexes and their bound target mRNAs. Rna. 2008;14: 2580–2596. doi:10.1261/rna.1351608

56. Davis TH, Cuellar TL, Koch SM, Barker AJ, Harfe BD, McManus MT, et al. Conditional loss of dicer disrupts cellular and tissue morphogenesis in the cortex and hippocampus. J Neurosci. 2008;28: 4322–4330. doi:10.1523/JNEUROSCI.4815-07.2008

57. Dörrbaum AR, Alvarez-Castelao B, Nassim-Assir B, Langer JD, Schuman EM. Proteome dynamics during homeostatic scaling in cultured neurons. Elife. 2020. doi:10.7554/eLife.52939

58. Jarome TJ, Werner CT, Kwapis JL, Helmstetter FJ. Activity dependent protein degradation is critical for the formation and stability of fear memory in the amygdala. PLoS One. 2011. doi:10.1371/journal.pone.0024349

59. Na Y, Park S, Lee C, Kim DK, Park JM, Sockanathan S, et al. Real-Time Imaging Reveals Properties of Glutamate-Induced Arc/Arg 3.1 Translation in Neuronal Dendrites. Neuron. 2016;91: 561–573. doi:10.1016/j.neuron.2016.06.017